Communications in Combinatorics and Optimization
Vol. 8, No. 1 (2023), pp. 207-241
DOI: 10.22049/CCO.2022.27346.1241

CCO
Commun. Comb. Optim.

Research Article

Signed bicyclic graphs with minimal index

Maurizio Brunetti*, **Adriana Ciampella**†

Dipartmento di Matematica e Applicazioni, University 'Federico II', Naples, Italy
*maurizio.brunetti@unina.it
†adriana.ciampella@unina.it

Received: 24 July 2021; Accepted: 6 January 2022
Published Online: 10 January 2022

Abstract: The index $\lambda_1(\Gamma)$ of a signed graph $\Gamma = (G, \sigma)$ is just the largest eigenvalue of its adjacency matrix. For any $n \geqslant 4$ we identify the signed graphs achieving the minimum index in the class of signed bicyclic graphs with n vertices. Apart from the $n = 4$ case, such graphs are obtained by considering a starlike tree with four branches of suitable length (i.e. four distinct paths joined at their end vertex u) with two additional negative independent edges pairwise joining the four vertices adjacent to u. As a by-product, all signed bicyclic graphs containing a theta-graph and whose index is less than 2 are detected.

Keywords: Signed Graph, Bicyclic Graph, Index, Extremal Graph Theory

AMS Subject classification: 05C22, 05C50, 15A18

1. Introduction

A *signed graph* $\Gamma = (G, \sigma)$ is a pair (G, σ), where $G = (V_G, E_G)$ is a simple graph and $\sigma \colon E_G \longrightarrow \{+1, -1\}$ is the sign function (or the *signature*) defined on the edge set of G. The unsigned graph G is called the *underlying graph* of Γ. The *order* and the *size* of Γ are the order and the size of its underlying graph. The *sign* of a cycle C in Γ is given by $\mathrm{sign}(C) = \prod_{e \in C} \sigma(e)$. If all edges in Γ are positive, then Γ is denoted by $(G, +)$. A cycle is called *positive* (resp., *negative*) if $\mathrm{sign}(C)$ is 1 (resp., -1). A signed graph is *balanced* if no negative cycles exist; otherwise it is *unbalanced*. The *negation* $-\Gamma$ is obtained by reversing the sign of every edge of Γ.
Most of the concepts defined for unsigned graphs are directly extended to signed graphs. For example, a signed graph is said to be *k-cyclic* if the underlying graph

* *Corresponding Author*

is k-cyclic. This means that G is connected and $|E_G| = |V_G| + k - 1$. We use the adjectives *unicyclic* and *bicyclic* as synonyms of 1-cyclic and 2-cyclic respectively.
The adjacency matrix A_Γ of $\Gamma = (G, \sigma)$ is obtained from the standard adjacency matrix A_G by replacing 1 by -1 whenever the corresponding edge is negative. By the *spectrum* of Γ, we mean the spectrum of A_Γ. Since A_Γ is symmetric, its eigenvalues $\lambda_1(\Gamma) \geqslant \lambda_2(\Gamma) \geqslant \cdots \geqslant \lambda_n(\Gamma)$ are real. Moreover, since the trace of A_Γ is equal to zero, we have $\lambda_1(\Gamma)\lambda_n(\Gamma) \leqslant 0$, with equality if and only if Γ is empty (without edges). The *index* of Γ is simply the largest eigenvalue $\lambda_1(\Gamma)$, whereas the *spectral radius* is the largest absolute value of its eigenvalues.
The 'spectral' sub-branch of extremal graph theory essentially consists in identifying those objects which are extremal with respect to a fixed spectral parameter within a given class of graphs. In the last few years, some extremal problems have been solved in the context of signed graphs. For instance, in [17] Koledin and Stanić studied connected signed graphs of fixed order, size and number of negative edges that maximize the index. In the wake of that paper, signed graphs maximizing the index in suitable subsets of complete signed graphs have been studied in [2, 13]. Let $\mathfrak{U}_n$ (resp., $\mathfrak{B}_n$) denote the class of unbalanced unicyclic (resp., bicyclic) signed graphs of order n. Akbari et al. [1] determined signed graphs with extremal index in the class $\mathfrak{U}_n$. Some of the same authors studied in [19] signed graphs achieving the maximum index among all graphs in $\mathfrak{U}_n$ of fixed girth. The first five largest indices among graphs in $\mathfrak{B}_n$ with $n \geqslant 36$ are detected by He et al. [14]. Signed graphs in $\mathfrak{U}_n$ and $\mathfrak{B}_n$ with extremal spectral radius were identified in [4]. Extremal graphs in $\mathfrak{U}_n$ and $\mathfrak{B}_n$ with respect to the least Laplacian eigenvalue were studied in [7] and [3], respectively. The first author and Stanić detected in [10] the signed graphs achieving the extremal spectral radii and the extremal indices in the set $\mathcal{U}_n$ of all unbalanced connected signed graphs with $n \geqslant 3$ vertices. Finally, the procedure in [10] to determine unbalanced graphs with largest index has been improved in [9], where it has been employed to find out the first few signed graphs ordered by the index in the class of connected signed graphs, or connected unbalanced signed graphs, or complete signed graphs.
This paper is devoted to prove that the signed graphs achieving the minimal index in $\mathfrak{B}_n$ for $n \geqslant 5$ are precisely those obtained by taking a starlike tree with four branches of suitable length, such graphs are obtained by considering four distinct paths joined at their end vertex u with two additional negative independent edges pairwise joining the four vertices adjacent to u (see Fig. 1). The length of each branch depends on the congruence class of n modulo 4 (see Theorem 2.1).
As made precise in Corollary 3.5, it follows that the same graphs also minimize the index in the class of all bicyclic graphs of given order.
The remainder of the paper is structured as follows. The main result, Theorem 2.1, is contained in Section 2 with some directions that help to guide one along the intermediate steps of the theorem's proof. Apart from fixing notation and terminology, Section 3 contains some basic tools of spectral graph theory and some bounds for the index of the possible index-minimizers. Results in Section 4 are all part of the proof of Theorem 2.1. For its completion, we employ a signless Laplacian variant of the celebrated Jacobs-Trevisan algorithm, originally defined to locate adjacency eigenvalues

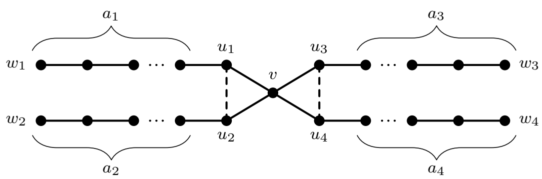

Figure 1. The signed graph Γ_{a_1,a_2,a_3,a_4}. Here and in the forthcoming figures, negative edges are depicted by dashed lines.

of trees. In fact, as made clear in Section 3, the indices of the signed graphs which seemingly are candidates to be index-minimizers (essentially, the graphs Γ_{a_1,a_2,a_3,a_4} and $\Gamma^p_{a_1,a_2,a_3,a_4}$ respectively depicted in Fig. 1 and Fig. 4), are related with the algebraic connectivity, i.e. the second smallest (signless) Laplacian eigenvalue, of several H-shape trees. Since the arguments to perform the algorithm are quite technical, they are postponed to Section 5.

2. Description of the main result

We now state the main result of this paper. The notion of switching equivalence is recalled in Section 3. For the definition of the signed graph Γ_{a_1,a_2,a_3,a_4}, see Fig. 1. Clearly, the order of Γ_{a_1,a_2,a_3,a_4} is $5 + \sum_{i=1}^4 a_i$. In particular, for $r > 0$, the signed graph

$$\Phi_{r,2} := \Gamma_{r,r-1,r-1,r-1} \tag{1}$$

has $4r + 2$ vertices.

Theorem 2.1. Let $\tilde{\Gamma}_n$ be a signed graph achieving the minimum index in the set $\mathfrak{B}_n$ of signed bicyclic graphs. Then:

i) $\tilde{\Gamma}_4$ is a diamond with two unbalanced triangles;

ii) $\tilde{\Gamma}_n$ with $n > 4$ is a switching equivalent to the signed graph

$$\Phi_{\{n\}} = \begin{cases} \Phi_{1,2} := \Gamma_{1,0,0,0} & \text{for } n = 6 \\ \widetilde{\Phi}_{r,2} := \Gamma_{r,r,r-1,r-2} & \text{for } n = 4r+2 \text{ and } r \geqslant 2, \\ \Phi_{r,3} := \Gamma_{r,r,r-1,r-1} & \text{for } n = 4r+3 \text{ and } r \geqslant 1, \\ \Phi_{r,4} := \Gamma_{r,r,r,r-1} & \text{for } n = 4r+4 \text{ and } r \geqslant 1, \\ \Phi_{r,5} := \Gamma_{r,r,r,r} & \text{for } n = 4r+5 \text{ and } r \geqslant 0. \end{cases} \tag{2}$$

The proof of Theorem 2.1 is long and requires many intermediate steps. In fact, it will only be completed in Section 5. Because of its intricacy, we give here a plan for the proof, describing how it is executed.

The case $n = 4$ is easy; therefore, we assume $n \geq 5$. Let P_k denote the (unsigned) path of order k. A first key result is given by the inequalities

$$\lambda_1(\Phi_{\{n\}}) < \lambda_1(P_{\nu_n+2}) = 2\cos\frac{\pi}{\nu_n+3} < 2, \quad \text{where } \nu_n := \left\lfloor \frac{n}{2} \right\rfloor \text{ (see Proposition 3.9),}$$

having two important consequences:

1. the diameter of $\tilde{\Gamma}_n$ cannot exceed ν_n (see Corollary 3.10);
2. the signed graph $\tilde{\Gamma}_n$ lies in the subset $\mathfrak{B}_n^*$ of bicyclic signed graphs of order n whose index is less than 2.

As better explained in Section 4, we regard $\mathfrak{B}_n^*$ as the union of the three disjoint subsets $\mathfrak{d}_n$, $\mathfrak{i}_n$ and $\mathfrak{th}_n$. Signed graphs in $\mathfrak{d}_n$ contain a dumbbell (two disjoint cycles joined by a non-trivial path); those in $\mathfrak{i}_n$ contain an ∞-graph (two cycles with just one vertex in common); those in $\mathfrak{th}_n$ contain a theta-graph (the union of three edge-disjoint paths of length $\geqslant 2$ between two vertices).
We shall prove that $\lambda_1(\Phi_{\{n\}}) < \lambda_1(\Theta)$ for each $\Theta \in \mathfrak{th}_n$ (see Theorem 4.7). Since $\Phi_{\{n\}}$ belongs to $\mathfrak{i}_n$, it follows that $\tilde{\Gamma}_n$ must be searched in $\mathfrak{d}_n \sqcup \mathfrak{i}_n$. The detection of index-minimizers in $\mathfrak{d}_n \sqcup \mathfrak{i}_n$ is performed in Section 4.1.
After noticing that all elements in $\mathfrak{d}_n \sqcup \mathfrak{i}_n$ have girth 3 and circumference $s \leqslant 5$, by separately analyzing the cases $s = 5$, $s = 4$ and $s = 3$ (which are *Case 1*, *2* and *3* respectively in Section 4.1), we discover that a signed graph in $\bigsqcup_{n\geq 5}(\mathfrak{d}_n \sqcup \mathfrak{i}_n)$ is switching equivalent to one of the items listed below:

1. a graph of type $\Gamma^p_{a_1,a_2,a_3,a_4}$ (see Fig. 4);
2. one of the graphs Γ_i ($1 \leqslant i \leqslant 16$) depicted in Fig. 5;
3. a graph of type $\Lambda^p_{h,k;\ell}$ (see Fig. 6);
4. a graph of type $X^p_{a_1,a_2,a_3,a_4}$ (see Fig. 7).

It turns out that index-minimizers are of type 1. In fact,

- a direct analysis is sufficient to show that no graph of type 2 is an index-minimizer (the several $\lambda_1(\Gamma_i)'s$ are listed in the Appendix);
- the only graphs of type 3 whose diameter is sufficiently small to be index-minimizers are $\Lambda^1_{0,0;0}$ of order 6, $\Lambda^1_{1,1;0}$ of order 8, and $\Lambda^1_{2,2;0}$ of order 10, but one easily checks that $\lambda_1(\Phi_{\{6\}}) < \lambda_1(\Lambda^1_{0,0;0})$, $\lambda_1(\Phi_{\{8\}}) < \lambda_1(\Lambda^1_{1,1;0})$, and $\lambda_1(\Phi_{\{10\}}) < \lambda_1(\Lambda^1_{2,2;0})$;
- no graphs of type 4 are index-minimizers by Proposition 4.5.

The proof ends by considering the only graphs of type 1 of order n whose diameter does not exceed ν_n. If n is odd, there is just $\Phi_{\{n\}}$, and there is nothing else to prove. If $n = 4r + 2$ (resp., $n = 4r + 4$) index-minimizers are in the set $\mathcal{G}_{4r+2} = \{\widetilde{\Phi}_{r,2}, \Phi_{r,2}, \Gamma^2_{r-1,r-1,r-1,r-1}, \Gamma^2_{r,r,r-2,r-2}\}$ (resp., $\mathcal{G}_{4r+4} = \{\Phi_{r,4}, \Gamma_{r+1,r,r-1,r-1}, \Gamma^2_{r,r,r-1,r-1}\}$).

Finally, in order to establish that only $\widetilde{\Phi}_{r,2}$ (resp. $\Phi_{r,4}$) minimizes the index in $\mathcal{G}_{4r+2}$ (resp., $\mathcal{G}_{4r+4}$) we compare the algebraic connectivities of some H-shaped graphs related to graphs in $\mathcal{G}_{4r+2} \cup \mathcal{G}_{4r+4}$ according to the formula (12). This comparison is performed in Section 5 by using the algorithm presented in Figure 12.

3. Basic tools and preliminaries

Let $\Gamma = (G, \sigma)$ be a signed graph. As usual, we denote by $\phi_A(G, \lambda) = \det(\lambda I_n - A_G)$ and $\phi_A(\Gamma, \lambda) = \det(\lambda I_n - A_\Gamma)$ the characteristic polynomial of A_G and A_Γ, respectively. In Section 4, we shall also consider the characteristic polynomial $\phi_Q(G, \lambda)$ of the signless Laplacian matrix $Q_G = D_G + A_G$, where D_G is the vertex degree matrix of G.

The first result we mention is very well-known and involves the spectrum of the (unsigned) path P_n with n vertices.

Proposition 3.1. [12, p. 73] The characteristic polynomial $\phi(P_n, \lambda)$ is equal to $U_n(\lambda/2)$, where $U_n(x)$ is the n-th Chebyshev polynomial of the second kind defined through the following identity
$$U_n(\cos \omega) \sin \omega = \sin((n+1)\omega).$$

Therefore, the eigenvalues of A_{P_n} are

$$\lambda_k(P_n) = 2 \cos \frac{k\pi}{n+1} \qquad \text{for } 1 \leqslant k \leqslant n.$$

For a signed graph $\Gamma = (G, \sigma)$ and a function $\theta \colon V_G \longrightarrow \{+1, -1\}$, we can build a new signed graph $\Gamma^\theta = (G, \sigma^\theta)$, where $\sigma^\theta(e) = \theta(v_i)\sigma(e)\theta(v_j)$ for each edge $e = v_i v_j \in E_G$. The signed graphs Γ and Γ^θ are said to be *switching equivalent*; they share the same spectrum and the same set of positive cycles. In fact, $A_{\Gamma^\theta} = D^{-1} A_\Gamma D$, where D is the diagonal matrix $\mathrm{diag}\,(\theta(v_1), \theta(v_2), \ldots, \theta(v_n))$. It can also be proved [21, Proposition 3.2] that two signed graphs sharing the same underlying graph are switching equivalent if and only if the set of balanced cycle is the same. This implies that Γ is balanced if and only if Γ is switching equivalent to $(G, +)$. In particular, any signed forest (F, σ) is balanced, the matrices $A_{(F,\sigma)}$ and A_F are similar and we denote their shared eigenvalues by $\lambda_1(F) \geqslant \cdots \geqslant \lambda_{|V_F|}(F)$.

For the same reason, all balanced (resp., unbalanced) cycles of fixed order are spectrally indistinguishable. With a slight abuse of notation we denote by C_n^b (resp., C_n^u) any balanced (resp., unbalanced) cycle of order $n \geqslant 3$.

We say that $\Lambda = (H, \tau)$ is an induced subgraph of $\Gamma = (G, \sigma)$, and write $\Lambda \subseteq \Gamma$, if H is an induced subgraph of G and $\tau = \sigma|_H$. Furthermore, we write $\Lambda \subset \Gamma$ and say that Γ *properly contains* Λ if $\Lambda \subseteq \Gamma$ and $H \neq G$.

Let $\Gamma - v$ denote the signed graph obtained from Γ by deleting the vertex v. The following result is known as the *Interlacing Theorem for Signed Graphs*, which is a consequence of the Cauchy Interlacing Theorem holding, in its general form, for principal submatrices of any Hermitian matrix (see [12, Theorem 0.10]).

Theorem 3.2. Let $\Gamma = (G, \sigma)$ be a signed graph of order $n \geqslant 2$, and let v be one of its vertices. The eigenvalues of A_Γ and those of $A_{\Gamma - v}$ interlace as follows:

$$\lambda_1(\Gamma) \geqslant \lambda_1(\Gamma - v) \geqslant \lambda_2(\Gamma) \geqslant \lambda_2(\Gamma - v) \geqslant \cdots \geqslant \lambda_{n-1}(\Gamma - v) \geqslant \lambda_n(\Gamma).$$

By using Theorem 3.2 the suitable number of times, we get the following corollary.

Corollary 3.3. If $\Lambda \subseteq \Gamma$ and Λ' is switching equivalent to Λ, then $\lambda_1(\Lambda') = \lambda_1(\Lambda) \leqslant \lambda_1(\Gamma)$.

The two parts of the following result respectively come from [1, Theorem 2.5] and [20, Lemma 2.1].

Theorem 3.4. The index of a signed graph $\Gamma = (G, \sigma)$ never exceeds $\lambda_1(G, +)$. Moreover, if Γ is connected, then $\lambda_1(\Gamma) = \lambda_1(G, +)$ if and only if Γ is balanced.

Theorem 3.4 has the following immediate consequence.

Corollary 3.5. Let $n \geq 4$. A signed graph $\tilde{\Gamma}_n$ minimizes the index among the signed bicyclic graphs of order n if and only if it is unbalanced and minimizes the index in $\mathfrak{B}_n$.

The next theorem encapsulates a Schwenk-like formula which will be repeatedly used along the paper.

Theorem 3.6. [6, Theorem 3.1] Let Γ be a signed graph and u be an arbitrary vertex of Γ. Then the following holds:

$$\phi(\Gamma, \lambda) = \lambda\, \phi(\Gamma - u, \lambda) - \sum_{u \sim v} \phi(\Gamma - u - v, \lambda) - 2 \sum_{C \in \mathcal{C}_u} \operatorname{sign}(C) \cdot \phi(\Gamma \setminus V(C), \lambda), \tag{3}$$

where $u \sim v$ means that u and v are adjacent and $\mathcal{C}_u$ is the set of cycles passing through u.

We now prove some bounds for the index of the graphs defined in (1) and (2).

Lemma 3.7. For $t \in \{1, 2\}$, the following inequalities hold:

$$2 \cos \frac{\pi}{2r + t + 2} < \lambda_1(\Phi_{r,2t}) \leqslant \lambda_1(\Phi_{r,2t+1}), \tag{4}$$

and

$$2 \cos \frac{\pi}{2r + 3} < \lambda_1(\widetilde{\Phi}_{r,2}) \leqslant \lambda_1(\Phi_{r,3}). \tag{5}$$

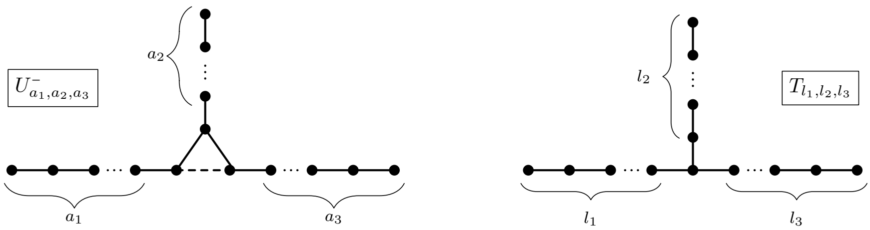

Figure 2. **The signed graph $U^-_{a_1,a_2,a_3}$ and the T-shape graph T_{l_1,l_2,l_3}**

Proof. Since $\Phi_{r,2t} \subseteq \Phi_{r,2t+1}$ and $\widetilde{\Phi}_{r,2} \subseteq \Phi_{r,3}$, the second inequalities of both (4) and (5) come from interlacing. Let now u_2 be the vertex of $\Phi_{r,2t}$ as in Fig. 1. The signed graph $\Phi_{r,2t} - u_2$ has two connected components. One is P_{r+t-2}. The other one is the signed unicyclic graph $U^-_{r+1,r+t-2,r-1}$ (see Fig. 2), whose index is strictly larger than $\lambda_1(P_{2r+t+1})$ (see [1, Theorem 3.4]). Thus, by interlacing,

$$2\cos\frac{\pi}{2r+t+2} < \lambda_1(U^-_{r+1,r+t-2,r-1}) \leqslant \lambda_1(\Phi_{r,2t}) \leqslant \lambda_1(\Phi_{r,2t+1}).$$

The argument to prove the first inequality of (5) is analogous. □

Lemma 3.8. For $t \in \{1,2\}$, $\lambda_2(\Phi_{r,2t+1}) = \lambda_1(P_{2r+2}) = 2\cos(\pi/(2r+3))$.

Proof. Let v the only vertex of $\Phi_{r,2t+1}$ of degree 4. We first deal with the case $t = 2$ which is easier. Since $\Phi_{r,5} - v = 2P_{2r+2}$, by Proposition 3.1 and Theorem 3.2 we arrive at

$$2\cos\frac{\pi}{2r+3} = \lambda_1(2P_{2r+2}) \geqslant \lambda_2(\Phi_{r,5}) \geqslant \lambda_2(2P_{2r+2}) = 2\cos\frac{\pi}{2r+3},$$

proving the statement for $t = 2$.
Let now $t = 1$. Note that $\Phi_{r,3} - v = P_{2r+2} \sqcup P_{2r}$. Therefore, by interlacing and (4), $\lambda_1(\Phi_{r,3}) > \lambda_1(P_{2r+2}) \geqslant \lambda_2(\Phi_{r,3})$. The proof will be over once we show that $\lambda_1(P_{2r+2})$ is an eigenvalue of $\Phi_{r,3}$.
If we use the Schwenk-like formula of Theorem 3.6 starting from the central vertex v of $\Phi_{r,3}$, we obtain

$$\begin{aligned}\phi(\Phi_{r,3};\lambda) = \phi(2r+2)\left(\lambda\phi(2r) - 2\phi(r)\phi(r-1) + 2\phi(r-1)^2\right) + \\ - 2\phi(2r)\phi(r)\left(\phi(r+1) - \phi(r)\right), \quad (6)\end{aligned}$$

where we set $\phi(k) = \phi(P_k;\lambda)$. From (6) it is immediately seen that

$$\phi(\Phi_{r,3};\lambda_1(P_{2r+2})) = 0 \iff \phi\left(P_{r+1};\lambda_1(P_{2r+2})\right) = \phi\left(P_r;\lambda_1(P_{2r+2})\right).$$

The latter equality actually holds and comes from Proposition 3.1. In fact, $\lambda_1(P_{2r+2}) = 2\cos\alpha$ for $\alpha = \frac{\pi}{2r+3}$, and

$$\phi\left(P_{r+1}; 2\cos\alpha\right) = \frac{\sin((r+2)\alpha)}{\sin\alpha} = \frac{\sin((r+1)\alpha)}{\sin\alpha} = \phi\left(P_r; 2\cos\alpha\right),$$

since $\sin((r+2)\alpha) = \sin(\pi - (r+1)\alpha) = \sin((r+1)\alpha)$. $\square$

Proposition 3.9. The indices of the signed graphs $\Phi_{r,\epsilon}$ and $\widetilde{\Phi}_{r,2}$ in (2) and (1) satisfy the following inequalities:

$$2\cos\frac{\pi}{2r+3} < \lambda_1(\Phi) < 2\cos\frac{\pi}{2r+4} \quad \text{for } \Phi \in \{\widetilde{\Phi}_{r,2}, \Phi_{r,2}, \Phi_{r,3}\}, \tag{7}$$

and

$$2\cos\frac{\pi}{2r+4} < \lambda_1(\Phi_{r,\epsilon}) < 2\cos\frac{\pi}{2r+5} \quad \text{for } \epsilon \in \{4,5\}. \tag{8}$$

Proof. The lower bounds of (7) and (8) immediately come from Lemma 3.7.
To prove the upper bounds, let $\beta = \pi/(2r+4)$ and $\gamma = \pi/(2r+5)$.
With the aid of Proposition 3.1, (6) and the software Wolfram|Alpha, the evaluation of $\phi(\Phi_{r,3}, \lambda)$ at $\lambda_1(P_{2r+3}) = 2\cos\beta$ gives

$$\phi\left(\Phi_{r,3}; 2\cos\beta\right) = \frac{32}{\sin^3\beta}\cdot\sin^7\frac{\beta}{2}\cdot\cos\frac{\beta}{2}\cdot\left(2\cos\beta+1\right)^2 \tag{9}$$

which is clearly a positive number. Since, by Lemma 3.8, $\lambda_2(\Phi_{r,3}) < 2\cos\beta$, the positivity of (9) and interlacing imply $\max\{\lambda_1(\widetilde{\Phi}_{r,2}), \lambda_1(\Phi_{r,2})\} \leqslant \lambda_1(\Phi_{r,3}) < 2\cos\beta$. Thus, (7) is proved.
The argument to prove the upper bound of (8) is similar. If we use the Schwenk-like formula (3) obtained by considering the central vertex v of $\phi(\Phi_{r,5}; \lambda)$ we arrive at

$$\phi(\Phi_{r,5}; \lambda) = \phi(2r+2)\left(\lambda\phi(2r+2) + 4\phi(r)(\phi(r) - \phi(r+1))\right), \tag{10}$$

where, once again, we set $\phi(k) := \phi(P_k; \lambda)$.
With the aid of Proposition 3.1, (10) and the software Wolfram|Alpha, the evaluation of $\phi(\Phi_{r,5}, \lambda)$ at $\lambda_1(P_{2r+4}) = 2\cos\gamma$ gives

$$\phi\left(\Phi_{r,5}; 2\cos\gamma\right) = 64\sin^6\frac{\gamma}{2}\cos^2\frac{\gamma}{2} > 0,$$

proving, together with Lemma 3.8, that the largest root of $\phi(\Phi_{r,5}, \lambda)$ – and *a fortiori* of $\phi(\Phi_{r,4}, \lambda)$ – is smaller than $2\cos\gamma$. Hence, the upper bound of (8) follows. $\square$

Table 1 in the Appendix involves the candidates to minimize the index in the several $\mathfrak{B}_n$'s for $5 \leqslant n \leqslant 9$. As many entries of Table 2, the values for the index from the second column of Table 1 on are approximated. Obviously, they are consistent with the bounds (7) and (8).

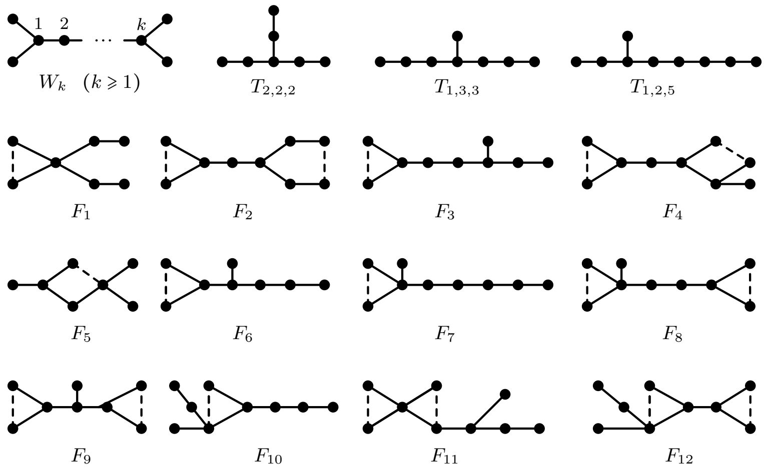

Figure 3. **Some forbidden graphs**

Corollary 3.10. The diameter of a signed graph minimizing the index in $\mathfrak{B}_n$ does not exceed $\nu_n := \lfloor \frac{n}{2} \rfloor$.

Proof. Let $\tilde{\Gamma}_n$ be a signed graph minimizing the index in $\mathfrak{B}_n$. If $\operatorname{diam} \tilde{\Gamma}_n = k-1$, then $\tilde{\Gamma}_n$ contains a signed path of order k and, by Corollary 3.3, $2\cos\frac{\pi}{k+1} = \lambda_1(P_k) \leq \lambda_1(\tilde{\Gamma}_n)$. The statement now follows by looking at the upper bounds of (7) and (8). ☐

The importance of Corollary 3.10 is transitory. In fact, ν_n is the diameter of the several $\Phi_{r,\epsilon}$'s and $\widetilde{\Phi}_{r,2}$'s . Therefore, Theorem 2.1, whose proof requires Corollary 3.10, will ensure that the diameter of index-minimizers in $\mathfrak{B}_n$ is precisely equal to ν_n.
Throughout the rest of the paper we say that a signed graph Λ is *forbidden* if and only if $\lambda_1(\Lambda) \geqslant 2$. The reason for this naming is readily explained. Let $\tilde{\Gamma}_n$ be a signed graph minimizing the index in $\mathfrak{B}_n$ for $n \geqslant 4$. From Proposition 3.9 and the fact that there are signed diamonds of order 4 whose index is less than 2, we immediately deduce that $\lambda_1(\tilde{\Gamma}_n) < 2$. Therefore, Corollary 3.3 implies that every forbidden signed graph cannot be contained in $\tilde{\Gamma}_n$. In particular, since $\lambda_1(C_n^b) = 2$, all graphs containing an induced balanced cycle are forbidden. Fig. 3 depicts a certain number of *minimal* forbidden signed graphs: in fact, their index is 2 and all their proper induced subgraphs have index in the interval $[0, 2)$. Graphs on the top row of Fig. 3, together with the cycles C_n, are known as *Smith graphs.*

We end this section by giving a rationale for the comparisons of algebraic connectivities performed in Section 5. Let G be an (unsigned) connected graph G with n vertices. We denote by $\mathcal{L}(G)$ its line graph, and by $0 \leqslant \mu_1(G) \leqslant \mu_2(G) \leqslant \cdots \leqslant \mu_n(G)$ the eigenvalues of Q_G. When G is a tree, the signless Laplacian eigenvalues are also the eigenvalues of $L_G = D_G - A_G$. Therefore, for every tree T, $\mu_1(T) = 0$ and $\mu_2(T) \neq 0$ is known as the *algebraic connectivity* of T.

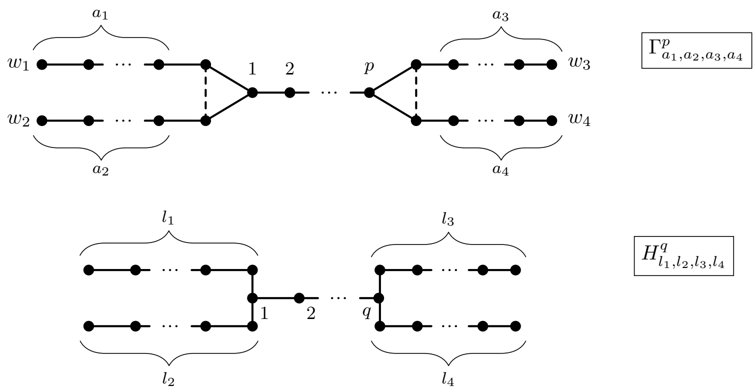

Figure 4. **The signed graph $\Gamma^p_{a_1,a_2,a_3,a_4}$ and the H-shape tree $H^q_{l_1,l_2,l_3,l_4}$**

Proposition 3.11. The following equalities hold:

$$\mu_2(T_{l_1,l_2,l_3}) = 2 - \lambda_1(U^-_{l_1-1,l_2-1,l_3-1}), \tag{11}$$

and

$$\mu_2(H^q_{l_1,l_2,l_3,l_4}) = 2 - \lambda_1(\Gamma^{q-1}_{l_1-1,l_2-1,l_3-1,l_4-1}), \tag{12}$$

where T_{l_1,l_2,l_3} is the T-shape graph depicted in Fig. 2, whereas $\Gamma^p_{a_1,a_2,a_3,a_4}$ and the H-shape tree $H^q_{l_1,l_2,l_3,l_4}$ are depicted in Fig. 4.

Proof. It is immediately seen that $\mathcal{L}(T_{l_1,l_2,l_3})$ and $\mathcal{L}(H^q_{l_1,l_2,l_3,l_4})$ are the underlying graphs of $U := U^-_{l_1-1,l_2-1,l_3-1}$ and $\Gamma = \Gamma^{q-1}_{l_1-1,l_2-1,l_3-1,l_4-1}$ respectively.
The signed graphs $-U$ and $-\Gamma$ are both balanced; therefore, they are spectral undistinguishable from their underlying graphs. Moreover, if n is the order of both U and Γ, then $\lambda_1(U) = \lambda_n(-U)$ and $\lambda_1(\Gamma) = \lambda_n(-\Gamma)$.
The equalities (11) and (12) now come from the well-known identity $\phi_A(\mathcal{L}(T), \lambda) = (\lambda+2)^{-1}\phi_Q(T, \lambda+2)$ holding for every tree T (see, for instance [11, Eq. 2]). $\square$

4. Chasing index-minimizers

The diamond, i.e. the graph made by two triangles sharing an edge, is the only bicyclic graph of order 4. By a direct calculation, the index of any diamond with two unbalanced triangles is $(\sqrt{17} - 1)/2 < 2$. Other types of diamonds contain at least one induced balanced triangle; hence, they are forbidden. This proves Part i) of Theorem 2.1.

From now on we assume $n \geqslant 5$. Note that there exists a unique pair $(r, \epsilon) \in \mathbb{N}_0 \times \{2, 3, 4, 5\}$ such that $n = 4r + \epsilon$. The proof consists in showing that if the signed bicyclic graph Γ belongs to $\mathfrak{B}_n$ and it is not switching equivalent to $\Phi_{\{n\}}$ defined in (2), then $\lambda_1(\Gamma) > \lambda_1(\Phi_{\{n\}})$. By Proposition 3.9, we can take into consideration only graphs in the set $\mathfrak{B}_n^*$ of bicyclic signed graphs of order n whose index is less than 2. As already observed in Section 3, a signed graph in $\mathfrak{B}_n^*$ does not contain any balanced cycle.

We recall that the *base* of a bicyclic graph $\Gamma = (G, \sigma)$, denoted by $\hat{\Gamma} = (\hat{G}, \sigma|_{\hat{G}})$, is the (unique) minimal bicyclic signed subgraph of Γ.

It is easy to verify that $\hat{\Gamma}$ is the unique bicyclic subgraph of Γ without pendant vertices (i.e. vertices of degree is 1), and Γ can be obtained from $\hat{\Gamma}$ by attaching signed trees to some vertices of $\hat{\Gamma}$.

The underlying graph $\hat{G}$ of $\hat{\Gamma}$ can be either a dumbbell, an ∞-graph, or a theta-graph. In other words, $\mathfrak{B}_n^* = \mathfrak{d}_n \sqcup \mathfrak{i}_n \sqcup \mathfrak{th}_n$, where

$$\mathfrak{d}_n := \{\Gamma \in \mathfrak{B}_n^* \mid \ \hat{G} \text{ is a dumbbell}\}, \qquad \mathfrak{i}_n := \{\Gamma \in \mathfrak{B}_n^* \mid \ \hat{G} \text{ is an } \infty\text{-graph}\},$$

and

$$\mathfrak{th}_n := \{\Gamma = (G, \sigma) \in \mathfrak{B}_n^* \mid \ \hat{G} \text{ is a theta-graph}\}.$$

The cases $\Gamma \in \mathfrak{d}_n \sqcup \mathfrak{i}_n$ and $\Gamma \in \mathfrak{th}_n$ will be dealt in two separate subsections.

4.1. Index-minimizers in $\mathfrak{d}_n \sqcup \mathfrak{i}_n$

Graphs in $\mathfrak{d}_n \sqcup \mathfrak{i}_n$ just contain two cycles, which are both unbalanced.

Let C_r^u and C_s^u (with $r \leqslant s$) be the two signed cycles contained in a signed graph $\Gamma \in \mathfrak{d}_{4r+\epsilon} \sqcup \mathfrak{i}_{4r+\epsilon}$. Once we set

$$\mathcal{D}(\Gamma) = \min\{d(v, w) \mid v \in C_r^u, w \in C_s^u\},$$

it is clear that a graph $\Gamma \in \mathfrak{d}_n \sqcup \mathfrak{i}_n$ belongs to $\mathfrak{i}_n$ if and only if $\mathcal{D}(\Gamma) = 0$.

Lemma 4.1. Let $\Gamma = (G, \sigma) \in \mathfrak{d}_n \sqcup \mathfrak{i}_n$. The two cycles of Γ have order $r = 3$ and $s \leqslant 5$.

Proof. Assume by contradiction that $r \geqslant 4$. In this case G would contain a double snake W_k (see Fig. 3) for a suitable $k \geqslant 1$, yet, double snakes are all forbidden. Therefore, $r = 3$. Now, $s \leqslant 5$, otherwise Γ would contain an induced subgraph switching equivalent to either $T_{2,2,2}$ or the graph F_1 of Fig. 3; yet, $T_{2,2,2}$ and F_1 are both forbidden. □

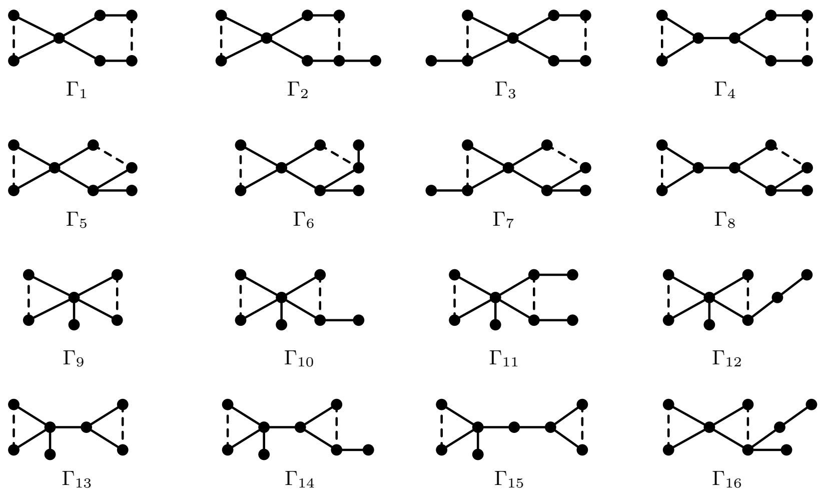

Figure 5. **Some graphs in $\mathfrak{i}_6$, $\mathfrak{i}_7$, $\mathfrak{i}_8$, $\mathfrak{d}_7$ and $\mathfrak{d}_8$**

Our investigation on graphs in $\mathfrak{d}_n \sqcup \mathfrak{i}_n$ will proceed from the biggest possible circumference (which is 5, by Lemma 4.1) to the smallest one (which is 3).

Case 1. $s = 5$.
Let C_3^u and C_5^u be the two unbalanced cycles of a signed graph $\Gamma = (G, \sigma)$ in $\mathfrak{d}_n \sqcup \mathfrak{i}_n$. Note that $\mathcal{D}(\Gamma) \leqslant 1$, otherwise Γ would contain a graph switching equivalent to one of the following forbidden graphs in Fig. 3: the graph F_2 if $\mathcal{D}(\Gamma) = 2$; the graph F_3 if $\mathcal{D}(\Gamma) = 3$; $T_{1,2,5}$ if $\mathcal{D}(\Gamma) > 3$.
A direct analysis shows that Γ is switching equivalent to one of the graphs Γ_i ($1 \leqslant i \leqslant 4$) depicted in Fig. 3. In fact, by adding to them an additional pendant vertex in every possible way, if the resulting signed graphs is not in $\{\Gamma_2, \Gamma_3, \Gamma_4\}$, then it is forbidden.

Case 2. $s = 4$.
Let C_3^u and C_4^u be the two unbalanced cycles of a signed graph $\Gamma = (G, \sigma)$ in $\mathfrak{d}_n \sqcup \mathfrak{i}_n$, and let $v \in C_3^u$ and $w \in C_4^u$ be the vertices such that $d(v, w) = \mathcal{D}(\Gamma)$. Clearly, v and w are the ending vertices of the (possibly trivial) path in $\hat{\Gamma}$ connecting the two cycles. We denote by w' and w'' the vertices in C_4^u adjacent to w, and by $d_G(u)$ the degree of a vertex u in G.

Subcase 2.1. $d_G(w')d_G(w'') > 4$.
As above, $\mathcal{D}(\Gamma) \leqslant 1$, otherwise Γ would contain a graph switching equivalent to one of the following forbidden graphs in Fig. 2: the graph F_4 if $\mathcal{D}(\Gamma) = 2$; the graph F_3 if $\mathcal{D}(\Gamma) = 3$; $T_{1,2,5}$ if $\mathcal{D}(\Gamma) > 3$. The non-forbidden signed graphs are switching equivalent to the graphs Γ_i ($5 \leqslant i \leqslant 8$) depicted in Fig. 5.

Subcase 2.2. $d_G(w')d_G(w'') = 4$.

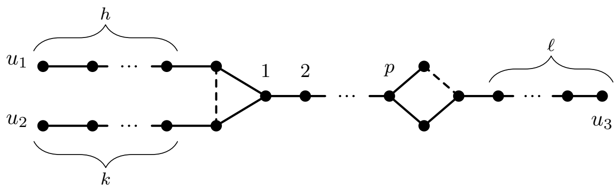

Figure 6. **The signed graph** $\Lambda^p_{h,k;\ell}$

Since the double snakes W_k's and F_5 are forbidden, the graph Γ is switching equivalent to a signed graph of type $\Lambda^p_{h,k;\ell}$, where $p = \mathcal{D}(\Gamma)+1$, $0 \leqslant h \leqslant k$, $\ell \geqslant 0$, with pendant vertices u_1,u_2 and u_3 (see Fig. 6). Since we are looking for possible index-minimizers, by Corollary 3.10 neither of the three distances $d(u_1,u_2)$, $d(u_1,u_3)$ and $d(u_2,u_3)$ should exceed $\nu_n = \lfloor \frac{n}{2} \rfloor$. This leads to the following algebraic constraints:

$$h+k \leq \nu_n - 1, \quad h+p+\ell \leq \nu_n - 2, \quad \text{and} \quad k+p+\ell \leq \nu_n - 2, \tag{13}$$

where $\ell = n-h-k-p-5$.
For even integers $n = 2q$, Conditions (13) are equivalent to

$$3 \leqslant q \leqslant 5, \quad q-3 \leqslant h \leqslant k, \quad h+k < q. \tag{14}$$

If instead $n = 2q+1$, Conditions (13) are only satisfied for $n = 7$, $h = 1$ and $k = 1$, but in this case ℓ would be negative.
There are only three graphs of type $\Lambda^p_{h,k;\ell}$ satisfying (14). Namely: $\Lambda^1_{0,0;0}$ of order 6, $\Lambda^1_{1,1;0}$ of order 8, and $\Lambda^1_{2,2;0}$ of order 10.

Case 3. $s = 3$.
Let Γ be a graph in $\mathfrak{d}_n \sqcup \mathfrak{i}_n$ containing two unbalanced triangles, and let P_Γ be the path connecting the two triangles in the base $\hat{\Gamma}$. Clearly, the order of P_Γ is $\mathcal{D}(\Gamma)+1$.

Subcase 3.1. There are some vertices in $V(\Gamma) \setminus V(\hat{\Gamma})$ adjacent to P_Γ.
Since the graphs $T_{1,3,3}$, F_6, F_7, and F_8 in Fig. 3 are forbidden, we have $\mathcal{D}(\Gamma) \leqslant 2$. The non-forbidden signed graphs are switching equivalent to the graphs Γ_i $(9 \leqslant i \leqslant 15)$ depicted in Fig. 5 (note that the graph F_9 in Fig. 3 is forbidden).

Subcase 3.2. There are no vertices in $V(\Gamma) \setminus V(\hat{\Gamma})$ adjacent to P_Γ. Since the double snakes W_k's, together with $T_{1,2,5}$, $T_{1,3,3}$ and the graphs F_{10}, F_{11} and F_{12} in Fig. 3 are forbidden, apart from graph Γ_{16} of Fig. 5, signed graphs of this type in $\mathfrak{d}_n \sqcup \mathfrak{i}_n$ are switching equivalent to an element in the set $\mathcal{S}'_n \cup \mathcal{S}''_n$, where

$$\mathcal{S}'_n = \{\Gamma^p_{a_1,a_2,a_3,a_4} \in \mathfrak{d}_n \sqcup \mathfrak{i}_n \mid p \geqslant 1,\ a_1 \geqslant a_2 \geqslant 0, \quad \text{and} \quad a_1 \geqslant a_3 \geqslant a_4 \geqslant 0\}$$

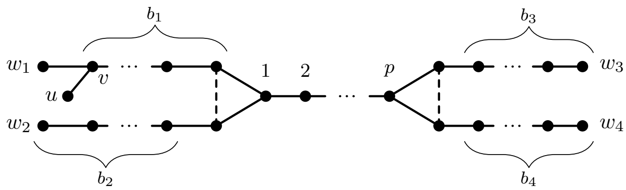

Figure 7. **The signed graph** $X^p_{b_1,b_2,b_3,b_4}$

and

$$\mathcal{S}''_n = \{X^p_{b_1,b_2,b_3,b_4} \in \mathfrak{d}_n \sqcup \mathfrak{i}_n \mid p \geqslant 1,\ b_1 \geqslant 0,\ b_2 \geqslant 0 \quad \text{and} \quad b_3 \geqslant b_4 \geqslant 0\}.$$

Elements in $\mathcal{S}'_n$ and in $\mathcal{S}''_n$ are respectively depicted in Figg. 4 and 7. Clearly, $\Gamma^1_{a_1,a_2,a_3,a_4}$ is precisely the graph Γ_{a_1,a_2,a_3,a_4} of Fig. 1. We first seek for index-minimizers in $\mathcal{S}'_n$. Note that every positive integer n can be uniquely written in the form

$$n = 2\nu_n + \omega, \qquad \text{where} \qquad \nu_n = \left\lfloor \frac{n}{2} \right\rfloor \quad \text{and} \quad \omega = \frac{1}{2}\left(1 + (-1)^n\right).$$

Clearly, $\omega \in \{0,1\}$ depends on the parity of n.

Lemma 4.2. If the diameter of $\Gamma^p_{a_1,a_2,a_3,a_4} \in \mathcal{S}'_n$ does not exceed ν_n, then

$$a_1 + a_3 = \nu_n - p - 1 \quad \text{and} \quad a_2 + a_4 = \nu_n + \omega - 3 \quad \text{with} \quad 1 \leqslant p \leqslant 2 - \omega. \tag{15}$$

Proof. Since $d(w_1, w_3) \leqslant \nu_n$ and $n = 2\nu_n + \omega = \sum_{i=1}^4 a_i + p + 4$, we can write

$$d(w_1, w_3) = a_1 + a_3 + p + 1 = \nu_n - k \quad \text{and} \quad a_2 + a_4 = \nu_n + \omega + k - 3 \tag{16}$$

for some $k \geqslant 0$. With Equations (16) at hand, the inequality $a_1 + a_3 \geqslant a_2 + a_4$ implies $2k + \omega \leqslant 2 - p \leqslant 1$, which is only possible for $k = 0$. Hence, $p \leqslant 2 - \omega$, and Equations (16) specialize to (15). □

By Corollary 3.10 and Lemma 4.2, we immediately realize that if $\Gamma^p_{a_1,a_2,a_3,a_4}$ minimizes the index in $\mathcal{S}'_{2\nu_n+\omega}$, then $(\omega, p) \in \{(0,1), (0,2), (1,1)\}$.

Subcase 3.2.1. $(\omega, p) = (0,1)$.
Equations (15) now read

$$a_1 + a_3 = \nu_n - 2 = (a_2 + a_4) + 1, \tag{17}$$

implying that $a_1 \geqslant (\nu_n - 2)/2$ and $a_2 \geqslant (\nu_n - 3)/2$. These two inequalities, together with $\nu_n \geqslant d(w_1, w_2) = a_1 + a_2 + 1$, give

$$\nu_n - 2 \leqslant a_1 + a_2 \leqslant \nu_n - 1.$$

By plugging $a_1 \geqslant a_2$ and $a_3 \geqslant a_4$ into (17) one at a time, we also obtain $a_{i+1} \leqslant a_i \leqslant a_{i+1} + 1$. for $i \in \{1, 3\}$. With these constraints at hand, it is now straightforward to check that $\Phi_{r,2}$ (for $r \geqslant 1$) and $\widetilde{\Phi}_{r,2}$ (for $r > 1$) are the only possible index-minimizers in $S'_{4r+2} \cap \mathfrak{i}_{4r+2}$. On the other hand, $\Phi_{r,4}$ and $\Gamma_{r+1,r,r-1,r-1}$ are the only possible index-minimizers in $S'_{4r+4} \cap \mathfrak{i}_{4r+4}$.

Subcase 3.2.2. $(\omega, p) = (0, 2)$.
Equations (15) become $a_1 + a_3 = \nu_n - 3 = a_2 + a_4$ which, together with $a_1 \geqslant a_2$ and $a_3 \geqslant a_4$ gives $a_1 = a_2$ and $a_3 = a_4$. From $d(w_1, w_2) = 2a_1 + 1 \leqslant \nu_n$ and $a_1 = \nu_n - a_3 - 3$ we arrive at

$$\frac{\nu_n - 5}{2} \leqslant a_3 = a_4 \leqslant a_1 = a_2 \leqslant \frac{\nu_n - 1}{2}. \tag{18}$$

It is straightforward to check that the only signed graphs in $\mathcal{S}'_{4r+2} \cap \mathfrak{d}_{4r+2}$ satisfying (18) are $\Gamma^2_{r,r,r-2,r-2}$ and $\Gamma^2_{r-1,r-1,r-1,r-1}$. In $\mathcal{S}'_{4r+4} \cap \mathfrak{d}_{4r+4}$, instead, constraints (18) are only satisfied by $\Gamma^2_{r,r,r-1,r-1}$.

Subcase 3.2.3. $(\omega, p) = (1, 1)$.
The argument is similar to the previous subcase. Equations (15) become $a_1 + a_3 = \nu_n - 2 = a_2 + a_4$ which, together with $a_1 \geqslant a_2$ and $a_3 \geqslant a_4$ gives $a_1 = a_2$ and $a_3 = a_4$. From $d(w_1, w_2) = 2a_1 + 1 \leqslant \nu_n$ and $a_1 = \nu_n - a_3 - 2$ we arrive at

$$\frac{\nu_n - 3}{2} \leqslant a_3 = a_4 \leqslant a_1 = a_2 \leqslant \frac{\nu_n - 1}{2}. \tag{19}$$

For $n = 4r + 3$, the sum $a_1 + a_3 = \nu_n - 2$ is odd; therefore, $a_1 \neq a_3$. Moreover, $(\nu_n - 3)/2 = r - 1$ and $(\nu_n - 1)/2 = r$. The only signed graph in $\mathcal{S}'_{4r+3}$ satisfying (19) is $\Phi_{r,3} = \Gamma_{r,r,r-1,r-1}$. For $n = 4r + 5$, instead, $(\nu_n - 2)/2 = r$, whereas the numbers $(\nu_n - 3)/2$ and $(\nu_n - 1)/2$ are not integers. Hence, the only integral 4-tuple (a_1, a_2, a_3, a_4) satisfying (19) is (r, r, r, r). In other words, the only index-minimizer in $\mathcal{S}'_{4r+5}$ is $\Phi_{r,5}$.

Proposition 4.3. For each $n \geqslant 5$ the set $\mathcal{S}'_n$ contains just one signed graph minimizing the index. Such graph is $\Phi_{\{n\}}$ defined in (2).

Proof. Subcase 3.2.3 analyzed above makes the statement trivial when n is odd. Let n be an even integer larger than 4. For $n = 6$, a direct check shows that $\lambda_1(\Phi_{1,2}) < \lambda_1(\Gamma^2_{0,0,0,0})$. For $n \geqslant 8$ we use Proposition 3.11 and the several comparison of algebraic connectivities performed in Section 5. More precisely, for $n = 4r + 2$ and $r > 1$, Propositions 5.6-5.8 will ensure that $\widetilde{\Phi}_{r,2}$ has the smallest index in the set

$$\{\widetilde{\Phi}_{r,2}, \Phi_{r,2}, \Gamma^2_{r-1,r-1,r-1,r-1}, \Gamma^2_{r,r,r-2,r-2}\}.$$

Similarly, for $n = 4r + 4$ and $r \geqslant 1$, Propositions 5.9 and 5.10 will suffice to prove that $\Phi_{r,4}$ minimizes the index in the set

$$\{\Phi_{r,4}, \Gamma_{r+1,r,r-1,r-1}, \Gamma^2_{r,r,r-1,r-1}\}. \qquad \square$$

The next step consists in showing that no graph in $\mathcal{S}''_n$ minimizes the index in $\mathfrak{d}_n \sqcup \mathfrak{i}_n$. Note that $\mathcal{S}''_n$ is nonempty for $n \geqslant 7$. Let Γ be a signed graph. For every eigenvalue λ of A_Γ, we denote by $\mathbf{y}_v$ the component of the λ-eigenvector $\mathbf{y}$ correspondent to a fixed vertex $v \in V(\Gamma)$.

Lemma 4.4. Let w be a pendant vertex of the index-minimizer $\tilde{\Gamma}'_n$ in $\mathcal{S}'_n$ for $n \geqslant 7$, and let $\mathbf{x}$ be a $\lambda_1(\tilde{\Gamma}'_n)$-eigenvector. Then, $\mathbf{x}_w$ is nonzero.

Proof. Let v, λ and $\mathbf{x}$ be a vertex of a signed graph Γ, an eigenvalue of A_Γ and a λ-eigenvector respectively. It is well known that if $\mathbf{x}_v = 0$, then λ is also an eigenvalue of $A_{\Gamma-v}$ (see, for instance, [16]). From the eigenvalue equations, we also see that if Γ is in $\mathcal{S}'_n$ and w is a pendant vertex such that $\mathbf{x}_w = 0$, then λ is also an eigenvalue of the graph obtained by cutting the vertices of the path connecting w to the base. This fact will be repeatedly used along all the cases. For terminology, we shall always refer to Fig. 1.

Case 1. $n = 4r + 2$ $(r \geqslant 2)$.
For $1 \leqslant i \leqslant 4$, the graphs $\widetilde{\Phi}_{r,2}(i)$'s obtained by removing from $\widetilde{\Phi}_{r,2} = \Gamma_{r,r,r-1,r-2}$ the path connecting w_i to u_i are all induced subgraph of $U^-_{r,r,r}$, whose index is $\lambda_1(P_{2r+2})$ (see [1, Theorem 3.4]). Yet, by interlacing and [1, Theorem 3.4]

$$\lambda_1(\widetilde{\Phi}_{r,2}) \geqslant \lambda_1(\widetilde{\Phi}_{r,2} - w_1) = \lambda_1(U^-_{r+1,r-1,r-2}) > \lambda_1(P_{2r+2}).$$

Hence, $\lambda_1(\widetilde{\Phi}_{r,2}) > \lambda_1(\widetilde{\Phi}_{r,2}(i))$ and $\mathbf{x}_{w_i} \neq 0$ for $1 \leqslant i \leqslant 4$.

Case 2. $n = 4r + 3$ $(r \geqslant 1)$.
Let λ be the index of $\Phi_{r,3} = \Gamma_{r,r,r-1,r-1}$, and let $\mathbf{x}$ be a λ-eigenvector. By symmetry, $\mathbf{x}_{w_1} = \mathbf{x}_{w_2}$, $\mathbf{x}_{u_1} = \mathbf{x}_{u_2}$ and $\mathbf{x}_{u_3} = \mathbf{x}_{u_4}$. Suppose that $\mathbf{x}_{w_1} = 0$. The eigenvalue equations show that $\mathbf{x}_{w_2} = \mathbf{x}_{u_1} = \mathbf{x}_{u_2} = \mathbf{x}_v = 0$ and $\mathbf{x}_{u_3} = -\mathbf{x}_{u_4}$. This should be possible only if all components of $\mathbf{x}$ were null, and this cannot occur. The cases $\mathbf{x}_{w_i} = 0$ for $i > 1$ are treated similarly.

Case 3. $n = 4r + 4$ $(r \geqslant 1)$.
For $1 \leqslant i \leqslant 4$, let $\Phi_{r,4}(i)$ be the graph obtained by removing from $\Phi_{r,4} = \Gamma_{r,r,r,r-1}$ the path connecting w_i to u_i. The graphs $\Phi_{r,4}(i)$ for $i < 4$ are all induced subgraph

of $U^-_{r,r,r}$, whose index is $\lambda_1(P_{2r+2})$ (see [1, Theorem 3.4]), whereas $\Phi_{r,4}(4) = U^-_{r+1,r,r}$. Yet, by Proposition 3.9, $\lambda_1(\Phi_{r,4}) > \lambda_1(P_{2r+2})$. This implies that $\lambda_1(\Phi_{r,4}) > \lambda_1(\Phi_{r,4}(i))$ for $i < 4$; therefore $\mathbf{x}_{w_i} \neq 0$ for $i < 4$. Now, suppose by contradiction that $\mathbf{x}_{w_4} = 0$. This would imply $\lambda_1(\Phi_{r,4}) = \lambda_1(U^-_{r+1,r,r})$ which, by (11) and (12), is equivalent to $\mu_2(H^2_{r+1,r+1,r+1,r}) = \mu_2(T_{r+2,r+1,r+1})$ against Corollary 5.5.

Case 4. $n = 4r + 5$ $(r \geqslant 1)$.
Let λ be the index of $\Phi_{r,5} = \Gamma_{r,r,r,r}$, and let $\mathbf{x}$ be a λ-eigenvector. By symmetry, if $\mathbf{x}_{w_j} = 0$ for some $j \in \{1, 2, 3, 4\}$ then $\mathbf{x}_{w_i} = 0$ for all $i \in \{1, 2, 3, 4\}$. Through the eigenvalue equation we shall infer that all components of $\mathbf{x}$ were null, and this is not possible. Hence, the statement is proved. □

Proposition 4.5. Let $n \geqslant 7$. For each signed graph Γ'' in $\mathcal{S}''_n$ there exists a graph $\tilde{\Gamma}'$ in $\mathcal{S}'_n$ such that $\lambda_1(\tilde{\Gamma}') < \lambda_1(\Gamma'')$.

Proof. Let $\Gamma'' := X^p_{b_1,b_2,b_3,b_4}$ a graph in $\mathcal{S}''_n$. We consider the graph $\Gamma' = \Gamma^p_{b+1,b_2,b_3,b_4}$ in $\mathcal{S}'_n$ obtained by replacing the positive edge uv with the positive edge uw_1 (see Fig. 7). We set $\lambda = \lambda_1(\Gamma')$ and consider a λ-eigenvector $\mathbf{x}$ of $A_{\Gamma'}$ with $\mathbf{x}_u \geqslant 0$. From the eigenvalue equations we deduce

$$\mathbf{x}_{w_1} = \lambda \mathbf{x}_u; \quad \text{and} \quad \mathbf{x}_v = \left(\lambda - \frac{1}{\lambda}\right)\mathbf{x}_{w_1}.$$

By definition, either $\Phi_{1,2}$ or the graph $U^-_{2,1,0}$ defined in [1] are induced subgraph of Γ'. Therefore, by interlacing, $\lambda > (\sqrt{5}+1)/2$. This implies that $\mathbf{x}_v \leqslant \mathbf{x}_{w_1}$. By [1, Lemma 2.8] it follows that $\lambda_1(\Gamma') \leqslant \lambda_1(\Gamma'')$, where the inequality is surely strict if $\mathbf{x}_u$ is nonzero. Now, if Γ' is an index-minimizer in $\mathcal{S}'_n$, then the statement comes from Lemma 4.4. Otherwise, there exists a $\tilde{\Gamma}'_n$ in $\mathcal{S}'_n$ such that $\lambda_1(\tilde{\Gamma}'_n) < \lambda_1(\Gamma') \leqslant \lambda_1(\Gamma'')$, as claimed. □

Proposition 4.6. For each $n \geqslant 5$, every index-minimizer in the set $\mathfrak{d}_n \sqcup \mathfrak{i}_n$ is switching equivalent to $\Phi_{\{n\}}$.

Proof. The case analysis performed in this subsection detected all potential index-minimizers. Let n_i be the order of the signed graph Γ_i in Fig. 5. Note that $n_i \leqslant 8$. From Table 2 in the Appendix we learn that $\lambda_1(\Phi_{\{n_i\}}) < \lambda_1(\Gamma_i)$ for $1 \leqslant i \leqslant 16$, $\lambda_1(\Phi_{\{6\}}) < \min\{\lambda_1(\Lambda^1_{0,0;0}, \lambda_1(\Gamma^2_{0,0,0,0})\}$ and $\lambda_1(\Phi_{\{8\}}) < \lambda_1(\Lambda^1_{1,1;0})$. Moreover, $\lambda_1(\Phi_{\{10\}}) < \lambda_1(\Lambda^1_{2,2;0}) = 1.93295$. The statement now comes from Propositions 4.3 and 4.5. □

4.2. A closer look to $\mathfrak{th}_n$

The entire subsection can be regarded as a proof of the following result.

Theorem 4.7. The inequality $\lambda_1(\Phi_{\{n\}}) < \lambda_1(\Theta)$ holds for each $n \geqslant 5$ and for each $\Theta \in \mathfrak{th}_n$.

It is immediately seen that Theorem 4.7 and Proposition 4.6, together with the introductory remarks at the beginning of Section 4, prove Theorem 2.1. Even when not explicitly stated, we always assume $n \geqslant 5$.

Lemma 4.8. Every $\Theta \in \mathfrak{th}_n$ has two unbalanced cycles sharing precisely one edge.

Proof. Suppose that the base $\hat{\Lambda}$ of a signed graph Λ of order n is a theta-graph. If $\hat{\Lambda}$ does not contain two unbalanced cycles sharing precisely one edge, then $\hat{\Lambda}$ (and Λ as well) contains as induced subgraph at least one balanced cycle. Thus, $\lambda_1(\Lambda) \geqslant 2$; hence, $\Lambda \notin \mathfrak{th}_n$. □

For $3 \leqslant r \leqslant s$, let $\Theta(C_r, C_s)$ denote the set of signed graphs whose base has two unbalanced cycles of order r and s sharing precisely one edge, and let $\mathfrak{th} = \bigcup_{n \geqslant 4} \mathfrak{th}_n$. We could rephrase Lemma 4.8 by saying that $\mathfrak{th} \subset \bigcup_{3 \leqslant r \leqslant s} \Theta(C_r, C_s)$.

Lemma 4.9. If $\mathfrak{th} \cap \Theta(C_r, C_s)$ is nonempty, then $r \leqslant 4$. Moreover, if $\mathfrak{th} \cap \Theta(C_4, C_s)$ is nonempty, then $s \leqslant 6$.

Proof. Let $5 \leqslant r \leqslant s$. The underlying graph of every $\Theta \in \Theta(C_r, C_s)$ contains the double snake W_1 (see Fig. 3) which is forbidden. For $s \geqslant 7$, a graph $\Theta \in \Theta(C_4, C_s)$ contains a subgraph switching equivalent to the forbidden graph F_{13} in Fig. 10. □

Up to switching equivalence, there are just eight signed graphs in $\mathfrak{th} \cap \bigcup_{4 \leqslant r \leqslant s \leqslant 6} \Theta(C_r, C_s)$. Referring to the notation of Fig. 8, we find

$$\Theta_i \in \begin{cases} \Theta(C_4, C_6) & \text{if } i = 1; \\ \Theta(C_4, C_5) & \text{if } 2 \leqslant i \leqslant 4; \\ \Theta(C_4, C_4) & \text{if } 5 \leqslant i \leqslant 8. \end{cases}$$

In fact, every signed graph obtained by adding an additional pendant vertex to an item in $\mathcal{T}_{(1)} = \{\Theta_i \mid 1 \leqslant i \leqslant 8\}$, if not in $\mathcal{T}_{(1)}$, has either $T_{1,3,3}$, $T_{2,2,2}$, a double snake, or a forbidden graph in $\{F_i \mid 13 \leqslant i \leqslant 16\}$ (see Fig. 10) among their induced subgraphs.
We now take into account the signed graphs in $\mathfrak{th}$ containing triangles.

Lemma 4.10. For each $s \geqslant 3$, $p \geqslant q \geqslant 0$ and $p \neq 0$, let $Z_{s;p}$ be the signed graph in Fig. 9, and let $\Delta_{p,q}$ and $\Delta'_{p,q}$ be the graphs in Fig. 11. Then,

(i) $\phi_A(Z_{s;p}, 2) = 4$;

(ii) $\phi_A(\Delta_{p,q}, 2) = 4$;

(iii) $\phi_A(\Delta'_{p,q}, 2) = 4 - pq$.

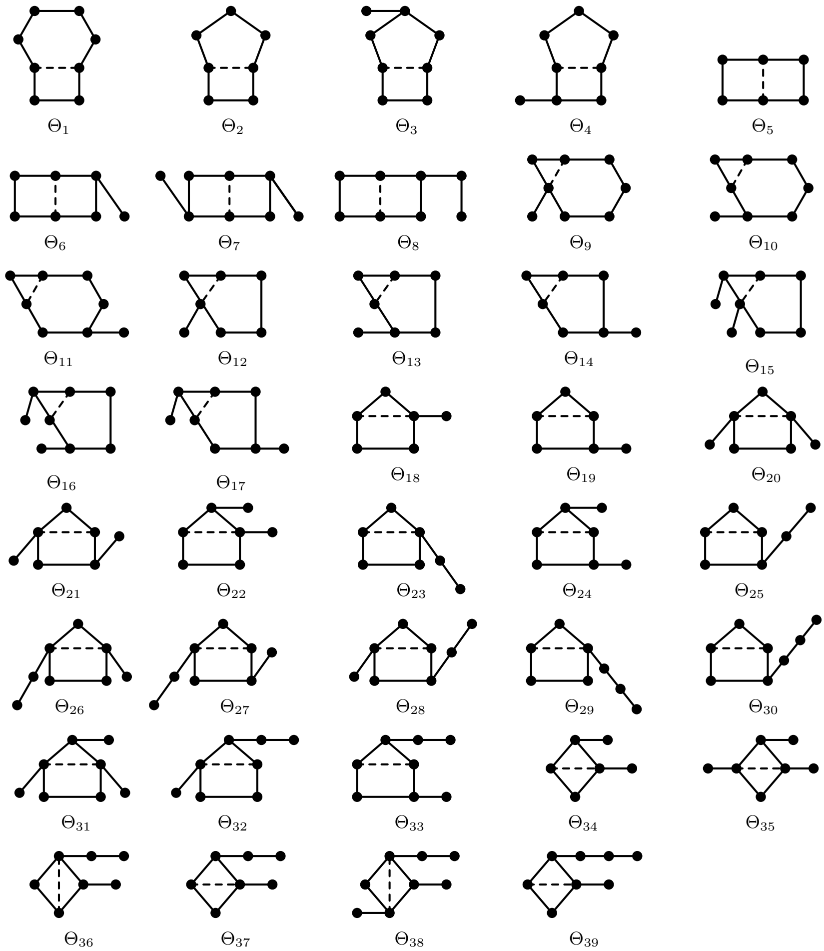

Figure 8. **Some graphs in $\mathfrak{th}_n$ for $6 \leqslant n \leqslant 8$.**

Figure 9. **The signed graphs $Z_{s;p}$ and $Z'_{s;p}$.**

Proof. Let Θ be a signed graph of type $Z_{s;p}$, $\Delta_{p,q}$, or $\Delta'_{p,q}$, and let w denote the vertex depicted in Figg. 9 and 11. The Schwenk decomposition (3) with respect to the vertex w (see Fig. 9) gives:

$$\begin{aligned}\phi(Z_{s;p}) = \lambda\phi(C^u_s)\phi(P_{p-1}) - 2\phi(P_{s-1})\phi(P_{p-1})\\ - \phi(P_{p-2})\phi(C^u_s) + 2\phi(P_{p-1})\phi(P_{s-2}) - 2\phi(P_{p-1}),\end{aligned} \quad (20)$$

$$\begin{aligned}\phi(\Delta_{p,q}) = \phi(P_p)\left(\lambda\phi(T_{1,1,q}) - 2\phi(P_{q+2})\right.\\ \left.-\phi(P_q)(\lambda^2 - 4\lambda + 2)\right) - \phi(P_{p-1})\phi(T_{1,1,q}),\end{aligned} \quad (21)$$

and

$$\begin{aligned}\phi(\Delta'_{p,q}) = \lambda\phi(P_{p+q+3}) - \phi(P_p)\left(\phi(P_{q+2}) - 2\phi(P_{q+1}) + 2\phi(P_q)\right)\\ - \phi(P_q)(\phi(P_{p+2}) - 2\phi(P_{p+1})) - \phi(P_{p+1})\phi(P_{q+1}),\end{aligned} \quad (22)$$

where $\phi(\Gamma)$ stands for $\phi_A(\Gamma, \lambda)$, $T_{1,1,0} := P_3$ and the pair $(\phi(P_0), \phi(P_{-1}))$ must be read as $(1, 0)$. By plugging in 20-22 $\phi_A(C^u_s, 2) = \phi(T_{1,1,q}, 2) = 4$ and $\phi_A(P_h, 2) = h + 1$, we easily arrive at the three equations in the statement. $\square$

Proposition 4.11. For each $s \geqslant 3$, $p \geqslant q \geqslant 0$ and $p \neq 0$, the graphs $Z_{s;p}$ and $\Delta_{p,q}$ belong to $\mathfrak{th}$, whereas the only graphs of type $\Delta'_{p,q}$ in $\mathfrak{th}$ are $\Delta'_{p,0}$, $\Delta'_{1,1}$ and $\Delta'_{2,1}$.

Proof. Let Θ be a signed graph of type $Z_{s;p}$, $\Delta_{p,q}$ or $\Delta'_{p,q}$, and let w denote the vertex depicted in Figg. 9 and 11. We observe that in all cases $\lambda_1(\Theta - w) < 2$. Since, by interlacing, $\lambda_2(\Theta) < 2$, the condition $\lambda_1(\Theta) < 2$ is equivalent to $\phi_A(\Theta, 2) > 0$. The statement now follows from Lemma 4.10. $\square$

It is worthwhile to notice that $\Delta'_{(p,0)} = Z_{3;p}$.

Proposition 4.12. For every $s \geqslant 3$ and $p \geqslant 1$, the index of the signed graphs $Z'_{s;p}$ in Fig. 9 is 2.

Proof. Let v be the vertex of $Z'_{s;p}$ as in Fig. 9. We set $Z_{s;0} := C^u_s$. By interlacing and Proposition 4.11, $\lambda_2(Z'_{s;p}) \leq \lambda_1(Z_{s;p-1}) < 2$. The statement will be proved once we show that $\phi_A(Z'_{s;p}, 2) = 0$. The Schwenk decomposition (3) with respect to the vertex v (see Fig. 9) gives:

$$\phi(Z'_{s;p}) = \begin{cases} \phi(Z_{s;p-1})(\lambda^3 - 2\lambda) - \lambda^2\phi(Z_{s;p-2}) & \text{if } p \geqslant 2, \\ \phi(C^u_s)(\lambda^3 - 2\lambda) - 2\lambda^2\left(\phi(P_{s-1}) - \phi(P_{s-2}) + 2\right) & \text{if } p = 1, \end{cases}$$

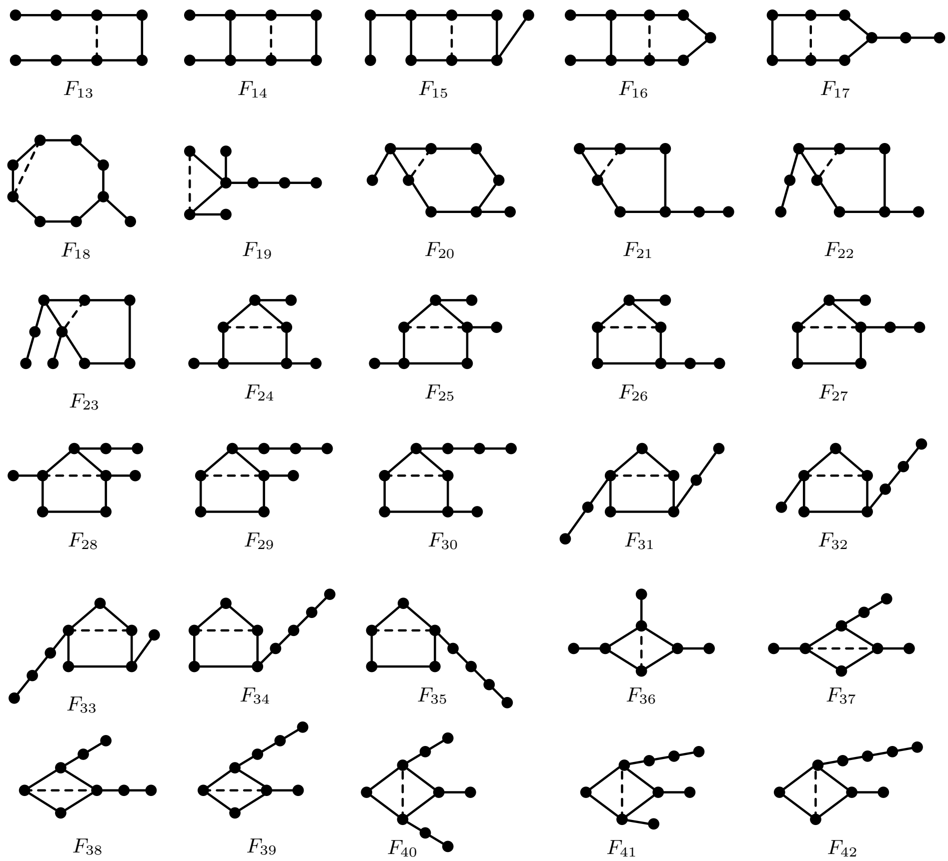

Figure 10. **Further forbidden graphs.**

where we have adopted the same convention as in the proof of Lemma 4.10 to denote characteristic polynomials. Recalling from Lemma 4.10 that $\phi_A(Z_{s;p-1}, 2) = \phi_A(C_s^u, 2) = 4$ for all $p \geqslant 1$, and knowing that $\phi(P_h, 2) = h + 1$, we see that 2 is indeed a root of the polynomial $\phi(Z'_{s;p})$. □

For $s \geqslant 3$, we now describe the set $\mathcal{U}_s := \Theta(C_3, C_s) \cap \mathfrak{th}$.

Lemma 4.13. For $s \geqslant 7$, every $\Theta \in \mathcal{U}_s$ is switching equivalent to $Z_{s;p}$ for some $p \geqslant 1$.

Proof. Let $s \geqslant 7$. If there exists a $\Theta \in \mathcal{U}_s$ which is not switching equivalent to any $Z_{s;p}$, then it contains a subgraph switching equivalent to either a graph of type $Z'_{s;q}$ or a forbidden graph in the set $\{T_{1,3,3}, F_6, F_{18}, F_{19}\}$. Hence, $\lambda_1(\Theta) \geqslant 2$. □

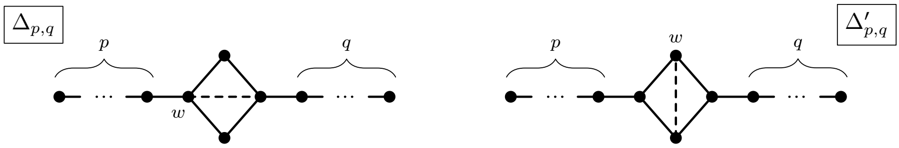

Figure 11. **The signed graphs $\Delta_{p,q}$ and $\Delta'_{p,q}$.**

Up to switching equivalence, it turns out that

(i) $\mathcal{U}_6 = \{\Theta_i \mid 9 \leqslant i \leqslant 11\} \cup \{Z_{6;p} \mid p \geqslant 1\}$ (see Figg. 8 and 9);

(ii) $\mathcal{U}_5 = \{\Theta_i \mid 12 \leqslant i \leqslant 14\} \cup \{Z_{5;p} \mid p \geqslant 1\}$;

(iii) $\mathcal{U}_4 = \{\Theta_i \mid 15 \leqslant i \leqslant 33\} \cup \{Z_{4;p} \mid p \geqslant 1\}$;

(iv) $\mathcal{U}_3 = \{\Theta_i \mid 34 \leqslant i \leqslant 39\} \cup \{Z_{3;p} \mid p \geqslant 1\} \cup \{\Delta_{p,q} \mid p \geqslant q \geqslant 0\} \cup \{\Delta'_{1,1}, \Delta'_{2,1}\}$.

In fact, up to switching equivalence, every signed graph obtained by adding an additional pendant vertex to an item in $\mathcal{T}_{(2)} = \{\Theta_i \mid 9 \leqslant i \leqslant 33\}$, if not in $\mathcal{T}_{(2)}$, contains a double snake, a graph of type $Z'_{s;q}$, or a forbidden graph in $\{T_{2,2,2}, F_1, F_6, F_{13}, F_i \mid 19 \leqslant i \leqslant 35\}$ (see Figg. 3 and 10). Similarly, every signed graph obtained by adding an additional pendant vertex to an item in $\mathcal{T}_{(3)} = \{\Theta_i \mid 9 \leqslant i \leqslant 35\}$, if not in $\mathcal{T}_{(3)}$, contains a double snake, a graph of type $Z'_{3;q}$, or a forbidden graph in $\{F_i, \Delta'_{p,q} \mid 36 \leqslant i \leqslant 42, pq = 4\}$.

The next proposition is the last result we need to prove Theorem 4.7.

Proposition 4.14. Let n be the order of $\Theta \in \{\Delta'_{1,1}, \Delta'_{2,0}, Z_{s;p}, \Delta_{p,q} \mid p \geqslant q \geqslant 0, p \neq 0\}$. If $\operatorname{diam} \Theta \leqslant \nu_n = \lfloor n/2 \rfloor$, then

(i) $\Theta \in \{Z_{4;1}, \Delta_{1,0}\}$ for $n = 5$;

(ii) $\Theta \in \{Z_{5;1}, Z_{4;2}, \Delta_{1,1}, \Delta_{2,0}\}$ for $n = 6$;

(iii) $\Theta \in \{Z_{n-1;1}, Z_{n-2;2}\}$ for even $n > 6$;

(iv) $\Theta \in \{Z_{n-1;1}\}$ for odd $n > 5$.

Proof. We immediately see that $\Delta'_{1,1}$ and $\Delta'_{2,0}$ have order 6 and diameter $4 > \nu_6 = 3$. Now, let $Z_{s;p}$ be a signed graph of order $n = 4r + \epsilon$ with $2 \leqslant \epsilon \leqslant 5$. It is not hard to check that

$$\operatorname{diam} Z_{s;p} = p + \left\lceil \frac{s}{2} \right\rceil - 1 = \begin{cases} p + k - 1 & \text{for even } s = 2k \\ p + k & \text{for odd } s = 2k + 1. \end{cases}$$

By studying separately the four cases

1) s even and $\epsilon \in \{2,3\}$, 2) s even and $\epsilon \in \{4,5\}$,
3) s odd and $\epsilon \in \{2,3\}$, 4) s odd and $\epsilon \in \{4,5\}$,

we discover that the conditions

$$s+p=n=4r+\epsilon \quad \text{and} \quad p+\left\lceil \frac{s}{2} \right\rceil -1 \leqslant \left\lfloor \frac{n}{2} \right\rfloor = \left\lfloor 2r+\frac{\epsilon}{2} \right\rfloor$$

are both satisfied only if $(s,p)=(n-1,1)$ and $(s,p)=(n-2,2)$ when n is even, and only if $(s,p)=(n-1,1)$ when n is odd. Analogously, since $\operatorname{diam}\Delta_{p,q}=p+q+1$, by distinguishing the cases $\epsilon \in \{2,3\}$ and $\epsilon \in \{4,5\}$, we check without difficulty that the conditions

$$|V_{\Delta_{p,q}}|=p+q+4=n=4r+\epsilon \quad \text{and} \quad p+q+1 \leqslant \left\lfloor \frac{n}{2} \right\rfloor = \left\lfloor 2r+\frac{\epsilon}{2} \right\rfloor$$

are only satisfied for $\epsilon=1$, $r=0$ and $(p,q)=(1,0)$, and $\epsilon=3$, $r=1$ and $p+q=2$, i.e. $(p,q)=(1,1)$ or $(p,q)=(2,0)$. □

We are now ready to finish the proof of Theorem 4.7. Summarizing the results gathered so far, we have proved that, up to switching equivalence,

$$\bigcup_{n\geqslant 5} \mathfrak{th}_n = \{\Theta_i, \mid 1 \leqslant i \leqslant 39\} \cup \{\Delta'_{1,1}, \Delta'_{2,1}, Z_{s;p}, \Delta_{p,q}, s \geqslant 3, p \geqslant q \geqslant 0, p \neq 0\}. \tag{23}$$

If we add to (23) the diamond $\Delta_{0,0}$ with four vertices and two unbalanced triangles we obtain the switching equivalence representatives of all signed bicyclic graphs whose base is a theta-graph and whose index is smaller than 2.

Denoted by n_i the order of Θ_i for $1 \leqslant i \leqslant 39$ in Fig. 8, from Table 4 in the Appendix we learn that $\lambda_1(\Phi_{(n_i)}) < \lambda_1(\Theta_i)$ for $1 \leqslant i \leqslant 39$. Now, by Corollary 3.10 and Proposition 4.6 we only need to check the inequalities $\lambda_1(\Phi_{\{s+p\}}) < \lambda_1(Z_{s;p})$ and $\lambda_1(\Phi_{\{p+q+4\}}) < \lambda_1(\Delta_{p,q})$ for the graphs listed in Proposition 4.14(i)-(iii). On Table 4 we read that $\lambda_1(\Phi_{\{6\}}) < \min\{\lambda_1(\Delta_{1,1}), \lambda_1(\Delta_{2,0})\}$. For the remaining signed graphs we distinguish three cases.

Case 1. $n=4r+2$.
For $r=1$, a direct computation shows that $\lambda_1(Z_{5;1})=1.75660$ and $\lambda_1(Z_{4;2})=1.81361$ are both larger than $\lambda_1(\Phi_{1,2})=1.67828$. For $r \geqslant 2$, we consider the vertex w in Fig. 9. By interlacing and Proposition 3.9, we arrive at

$$\lambda_1(Z_{4r+1;1}) \geqslant \lambda_1(Z_{4r+1;1}-w) = \\ \lambda_1(C^u_{4r+1}) = 2\cos\frac{\pi}{4r+1} > 2\cos\frac{\pi}{2r+4} > \lambda(\Phi_{\{4r+2\}}),$$

and

$$\lambda_1(Z_{4r;2}) \geqslant \lambda_1(Z_{4r;2} - w) = \lambda_1(C^u_{4r}) = 2\cos\frac{\pi}{4r} \geqslant 2\cos\frac{\pi}{2r+4} > \lambda(\Phi_{\{4r+2\}}).$$

Case 2. $n = 4r + 4$.
Again by interlacing and Proposition 3.9, we see that

$$\lambda_1(Z_{4r+3;1}) \geqslant \lambda_1(Z_{4r+3;1} - w) = \lambda_1(C^u_{4r+3}) = 2\cos\frac{\pi}{4r+3} \geqslant 2\cos\frac{\pi}{2r+5} > \lambda(\Phi_{\{4r+4\}}), \quad \text{for all } r \geqslant 1.$$

Moreover,

$$\lambda_1(Z_{4r+2;2}) \geqslant \lambda_1(Z_{4r+2;2} - w) = \lambda_1(C^u_{4r+2}) = 2\cos\frac{\pi}{4r+2} \geqslant 2\cos\frac{\pi}{2r+5} > \lambda(\Phi_{\{4r+4\}}), \quad \text{for all } r \geqslant 2.$$

Finally, for $r = 1$, $\lambda_1(Z_{6;2}) = 1.87228 > 1.76893 = \lambda(\Phi_{\{8\}})$.
Case 3. $n = 4r + 2t + 1$ with $t \in \{1, 2\}$.
Arguing as above,

$$\lambda_1(Z_{4r+2t;1}) \geqslant \lambda_1(Z_{4r+2t;1} - w) = \lambda_1(C^u_{4r+2t}) = 2\cos\frac{\pi}{4r+2t} \geqslant 2\cos\frac{\pi}{2r+3+t} > \lambda(\Phi_{\{4r+2t+1\}}).$$

5. A comparison of algebraic connectivities

In this section we compare the algebraic connectivity of some pairs of graphs of type T_{l_1,l_2,l_3} or $H^q_{l_1,l_2,l_3,l_4}$ (see Figg. 2 and 4). The main tools for doing that is the algorithm presented in Figure 12, which may be used to determine the number of Q-eigenvalues of a given tree in any interval. It is a Q-variant of the Jacobs-Trevisan algorithm [15] originally devised for the adjacency matrix. Recently, such Q-variant has been successfully employed to compare Q-indices of quipus [5]. The algorithm is based on the diagonalization of the matrix $Q(T)+\alpha I$, where α is a given real number. In fact, it produces a diagonal matrix D congruent to $Q(T) + \alpha I$. Consequently, the following result holds.

Theorem 5.1. [5, Theorem 3.1] Let T be a tree and consider *Diagonalize*$(T, -\alpha)$. Let $(d_v)_{v\in V(T)}$ be the sequence it produces. Then, the diagonal matrix $D = \mathrm{diag}(d_v)_{v\in V(T)}$ is congruent to $Q(T) - \alpha I$. So the number of (positive | negative | zero) entries in $(d_v)_{v\in V(T)}$ is equal to the number of eigenvalues of $Q(T)$ that are (greater than α | smaller than α | equal to α).

Figure 12. **The algorithm** ***Diagonalize***$(T, -\alpha)$.

Input: tree T, scalar α
Output: diagonal matrix D congruent to $A(T) + \alpha I$

Algorithm Diagonalize(T, α)
    initialize $d(v) := \deg(v) + \alpha$, for all vertices v
    order vertices bottom up
    for $k = 1$ to n
        if v_k is a leaf **then** continue
        else if $d(c) \neq 0$ for all children c of v_k **then**
            $d(v_k) := d(v_k) - \sum \frac{1}{d(c)}$, summing over all children of v_k
        else
            select one child v_j of v_k for which $d(v_j) = 0$
            $d(v_k) := -\frac{1}{2}$
            $d(v_j) := 2$
            if v_k has a parent v_l, remove the edge $v_k v_l$.
    end loop

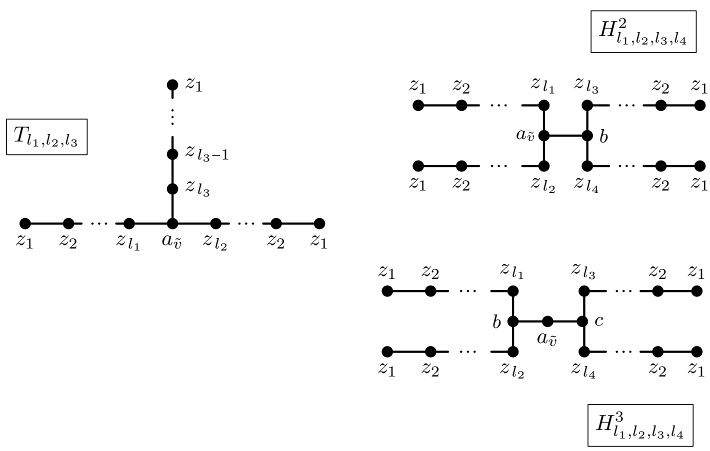

Figure 13. **Valued** T**-shape and** H**-shape trees after running the algorithm**

Note that the algorithm requires the choice in T of a root $\tilde v$, which is the last vertex to be processed. For each $v \neq \tilde v$, the final output d_v is given by the value $d(v)$ computed on line 6 of the algorithm if $d(v) \neq 0$. The types of trees on which the algorithm will be implemented are depicted in Fig. 13.

Lemma 5.2. Let T be one of the trees in Fig. 13, and let l be the maximum among the labels of the z_i's involved. Once we execute *Diagonalize*$(T, -\alpha)$ with $0 < \alpha < 1$, and $z_h > 0$ for a fixed $h \leqslant l - 1$, then $z_{h+1} < z_h$.

Proof. By choosing as root the vertex $\tilde{v}$ with output $a_{\tilde{v}}$, we arrive at the following recursive relations

$$\begin{cases} z_1 = 1-\alpha \\ z_{i+1} = 2-\alpha-\frac{1}{z_i}, \qquad i=1,\dots,l-1. \end{cases}$$

If $z_i > 0$, the inequality $z_{i+1} < z_i$ is equivalent to $z_i^2-(2-\alpha)z_i+1>0$, which actually holds. In fact, $\Delta=(2-\alpha)^2-4$ is negative. □

The following lemma is known to the experts and it is a consequence of [18, Theorem 3.1].

Lemma 5.3. Let T and T' be two trees. If $T\subseteq T'$, then $\mu_2(T)\geqslant\mu_2(T')$.

Proposition 5.4. For each $r\geqslant 1$, $\mu_2(T_{r+2,r+1,r+1})>\mu_2(H^2_{r+1,r+1,r+1,1})$.

Proof. Let $T:=T_{r+2,r+1,r+1}$, $T'=H^2_{r+1,r+1,r+1,1}$ and $T''=T_{3,2,2}$. Since $T''\subseteq T\subset T'$, by Lemma 5.3 or, equivalently, by Proposition 3.11 and interlacing,

$$\mu_2(T')\leqslant\mu:=\mu_2(T)\leqslant\mu_2(T'')=0.2434. \tag{24}$$

In order to show that the first inequality in (24) is strict, we are going to execute *D:=Diagonalize*$(T,-\mu)$ first, and D'=*Diagonalize*$(T',-\mu)$ afterwards. Our claim will be proved once we show that D' provides at least two negative outputs. In the case at hand, the graph on the left of Fig. 13 has $(z_{l_1},z_{l_2},z_{l_3})=(z_{r+2},z_{r+1},z_{r+1})$. Since T has only one Q-eigenvalue less than $\mu_2(T)$, at its completion the algorithm D produces (at least) a zero and exactly one negative output. Whilst the D is processing, the case $z_i=0$ for some i cannot occur. In fact, the appearance of 0 among $z_1,\dots,z_{r+1}$ would produce two negative outputs, and $z_{r+2}=0$ (once we know that $z_i\neq 0$ for $i<r+2$) would produce no zero outputs. Hence, $z_{r+2}<0$ and

$$a_{\tilde{v}}(T)=(3-\mu)-\frac{2}{z_{r+1}}-\frac{1}{z_{r+2}}=0. \tag{25}$$

By plugging in (25) $z_{r+2}=2-\mu-z_{r+1}^{-1}$, it turns out that z_{r+1} is the smallest root of $(5-5\mu+\mu^2)x^2-(7-3\mu)x+2$, i.e.

$$z_{r+1}=\frac{7-3\mu-\sqrt{9-2\mu+\mu^2}}{2(5-5\mu+\mu^2)}. \tag{26}$$

From $z_{r+2}=z_{r+1}((2-\mu)z_{r+1}-1)^{-1}<0$, we deduce $z_{r+1}<(2-\mu)^{-1}$, therefore, when we execute D', the output correspondent to the non-root of degree 3 is

$$b=3-\mu-\frac{1}{z_{r+1}}-\frac{1}{z_1}<3-\mu+(\mu-2)-(1-\mu)^{-1}=-\mu/(1-\mu)<0,$$

and with the aid of Wolfram|Alpha we discover that the output at the root of T'

$$(3-\mu)-\frac{2}{z_{r+1}}-\frac{1}{b}=(3-\mu)-\frac{2}{z_{r+1}}+\frac{(1-\mu)z_{r+1}}{(1-\mu)-(2-4\mu+\mu^2)z_{r+1}}$$

is negative as well for $\mu \in (0, 0.25)$ when we plug (26) in it. □

Corollary 5.5. For each $r \geqslant 1$, $\mu_2(T_{r+2,r+1,r+1}) > \mu_2(H^2_{r+1,r+1,r+1,r})$.

Proof. Since $H^2_{r+1,r+1,r+1,1} \subseteq H^2_{r+1,r+1,r+1,r}$, from Lemma 5.3 and Proposition 5.4 we immediately obtain

$$\mu_2(T_{r+2,r+1,r+1}) > \mu_2(H^2_{r+1,r+1,r+1,1}) \geqslant \mu_2(H^2_{r+1,r+1,r+1,r}). \qquad \square$$

The next three propositions compare the algebraic connectivity of H-shape trees with $4r+3$ vertices.

Proposition 5.6. For each $r \geqslant 2$, $\mu_2(H^2_{r+1,r,r,r}) < \mu_2(H^2_{r+1,r+1,r,r-1})$.

Proof. We set $T(r) := H^2_{r+1,r,r,r}$, $T'(r) := H^2_{r+1,r+1,r-1,r-2}$, and $\mu := \mu_2(T(r))$. For $r \in \{2, 3\}$ the statement comes from a direct computation.
Let $r \geqslant 4$. The proof first requires the execution of D:=*Diagonalize*$(T(r), -\mu)$. Since $T(4) \subseteq T(r)$, Lemma 5.3 yields $\mu := \mu_2(T(r)) \leqslant \mu_2(T(4)) = 0.07165 < 0.0844$. The importance of this bound will be clear later on.
Note that D produces (at least) one zero output and just one negative final value; therefore, $z_i > 0$ for $0 \leqslant i \leqslant r$. We also have $z_{r+1} = (2-\mu) - z_r^{-1} > 0$. Otherwise $z_r^{-1} \leqslant 2-\mu$, and D would produce at least two negative outputs: one along the first H-ray (or at the root if $z_{r+1} = 0$) and

$$b = 3-\mu-2z_r^{-1} \leqslant (3-\mu)-(4-2\mu) < 0.$$

When b is firstly processed, it cannot be zero. Otherwise the outputs at the two vertices of degree 3 would be 2 and $-1/2$, and no zero output would come out.
So far, we have proved that $z_i > 0$ for $1 \leqslant i \leqslant r+1$ and $b = 3-\mu-2z_r^{-1} < 0$. From $z_{r+1} > 0$ and $b < 0$, we deduce

$$(2-\mu)^{-1} < z_r < 2(3-\mu)^{-1}. \tag{27}$$

A straightforward manipulation shows that $a(\tilde{v}) = 3-\mu-z_r^{-1}-z_{r+1}^{-1}-b^{-1}$ is zero if and only if $f_\mu(z_r) = 0$, where

$$f_\mu(x) = (13-19\mu+8\mu^2-\mu^3)x^3-(24-21\mu+4\mu^2)x^2+(13-5\mu)x-2. \tag{28}$$

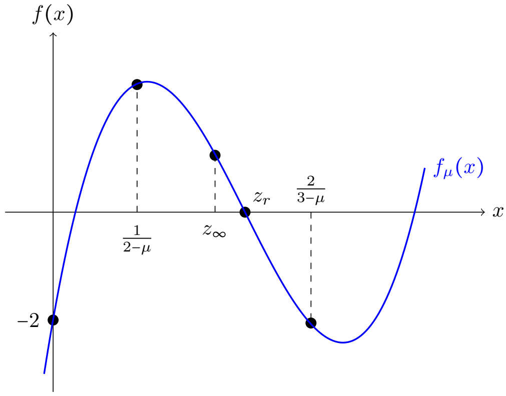

Figure 14. **The function** $f_\mu(x)$

As a consequence of (7) and (12), when $r \to \infty$, μ tends to 0. Thus, by (27) and (28), z_r tends to $z_\infty = (11+\sqrt{17})/26$, which is the only root of $f_0(x)$ in the interval $(1/2, 3/2)$. Condition $\mu < 0.0844$ (holding for $r \geqslant 4$) ensures that z_∞ belongs to the interval $(1/(2-\mu),\ 2/(3-\mu))$. Moreover,

$$f_\mu(z_\infty) = -\frac{1}{4394}\Big((95\sqrt{17}+473)\mu^2 - 4(47\sqrt{17}+49)\mu - (353\sqrt{17}+555)\Big)$$

is positive and belongs to the interval $(0.0458, 0.052)$. The contour plot of the function $f_\mu(x)$ is sketched in Fig. 14. It takes into account the equalities $f_\mu(1/(2-\mu)) = (1-\mu)/(2-\mu)^3 > 0$ and $f_\mu(2/(3-\mu)) = -4(1-\mu)/(3-\mu)^3 < 0$.
Since the number

$$f_\mu\left(\frac{\sqrt{5}-1}{2}\right) = -\frac{1}{2}\Big(2(\sqrt{5}-2)\mu^3 + 4(11-5\sqrt{5})\mu^2 + 16(4\sqrt{5}-9)\mu - 63\sqrt{5}+141\Big)$$

is negative for $\mu < 0.0844$, we also infer by Fig. 14 that

$$0 < z_\infty < z_r < (\sqrt{5}-1)/2. \tag{29}$$

We now consider the graph $T'(r)$ and execute $D' := \mathit{Diagonalize}(T'(r), -\mu)$, proving that it just gives one negative output; namely $b(T')$. We already know that the z_i's are all positive for $1 \leqslant i \leqslant r+1$, and

$$\begin{aligned} b(T') &= 3-\mu - z_r^{-1} - z_{r-1}^{-1} = 3-\mu-z_r^{-1}+z_r-(2-\mu) \\ &= z_r^{-1}(z_r^2+z_r-1). \end{aligned}$$

This number is negative by (29). The output corresponding to the root is

$$a_{\tilde{v}}(T') = 3 - \mu - 2z_{r+1}^{-1} - b(T')^{-1} = \frac{\Omega(z_r)}{(z_r^2 + z_r - 1)((2-\mu)z_r + 1)}$$

where

$$\Omega(x) = (\mu^2 - 5\mu + 4)x^3 + (\mu^2 - 3\mu + 1)x^2 - (\mu^2 - 6\mu + 6)x + 3 - \mu.$$

The proof will be over once we show that $a_{\tilde{v}}(T') > 0$ or, equivalently, $\Omega(z_r) < 0$. By the Descartes's rule of signs, the polynomial $\Omega(x)$ has two positive roots, but only one of them belongs to the interval $((2-\mu)^{-1}, 1)$, since

$$\Omega(1/(2-\mu)) = 2(2-\mu^3)(\mu^3 - 3\mu + 1) > 0, \quad \text{and} \quad \Omega(1) = -\mu(3-\mu) < 0.$$

With the aid of Wolfram|Alpha, we compute

$$\Omega(z_\infty) = -\frac{1}{4394}\left(3(23\sqrt{17} - 163)\mu^2 + 2(55\sqrt{17} + 852)\mu - 777\sqrt{17} + 3023\right)$$

which is negative for $\mu < 0.0844$. As claimed, $\Omega(z_r) < 0$. In fact,

$$z_r \in \left(z_\infty, 2(3-\mu)^{-1}\right) \subset (z_\infty, 1),$$

an interval along which $\Omega(x)$ is always negative. $\square$

Proposition 5.7. For each $r \geqslant 1$, $\mu_2(H^2_{r+1,r,r,r}) > \mu_2(H^3_{r,r,r,r})$.

Proof. A direct check suffices to prove the statement for $r \in \{2,3\}$. Let now $r \geqslant 4$. We set once again $\mu := \mu_2(H)$, where $H =: H^2_{r+1,r,r,r}$ and use some results obtained along the previous proof to execute $D_{H'}$:=*Diagonalize*$(H', -\mu)$, where $H' := H^3_{r,r,r,r}$ (see the H-shape tree on the right in Fig. 13). In fact, we already know that $z_i > 0$ for all $i \leqslant r+1$, and $b(H) := 3 - \mu - 2z_r^{-1} < 0$. Now, the numbers $b(H')$ and $c(H')$ correspondent to the two vertices of degree 3 in H' are both equal to $b(H)$. The presence of at least two negative outputs for $D_{H'}$ prove the statement. $\square$

Proposition 5.8. For each $r \geqslant 2$, $\mu_2(H^2_{r+1,r+1,r,r-1}) > \mu_2(H^3_{r+1,r+1,r-1,r-1})$.

Proof. We set $\tilde{T}(r) := H^2_{r,r-1,r+1,r+1}$ (the root we are choosing is adjacent to H-rays of different length), $\tilde{T}'(r) := H^3_{r+1,r+1,r-1,r-1}$, and $\mu := \mu_2(\tilde{T}(r))$. Since $\mu_2(\tilde{T}(2)) = 0.18216$, by Lemma 5.3 we know that $\mu \leqslant 0.18216$ for every $r \geqslant 2$.

The proof first requires the execution of $\tilde{D}$:=*Diagonalize*($\tilde{T}(r), -\mu$). Since many arguments are similar to the ones used along the proof of Proposition 5.6, we shall skip some details. We know that among the final values produced by $\tilde{D}$ at least one is zero and precisely one is negative; therefore $z_i > 0$ for all $i \leqslant r$. Note that z_{r+1} is positive as well: if along the process $z_{r+1} = 0$, then the final outputs at the two vertices of degree 3 would be both negative.
Now, by Lemma 5.2, the numbers

$$b(\tilde{T}(r)) = 3 - \mu - 2z_{r+1}^{-1} = \frac{z_r}{z_r^2 + z_r - 1} \tag{30}$$

and $3-\mu-z_r^{-1}-z_{r-1}^{-1}$ cannot be both zero. Thus, $b(\tilde{T}(r))$ is the (necessarily negative) output correspondent to the non-root vertex of degree 3, whereas the output at the root is

$$a_{\tilde{v}}(\tilde{T}(r)) = 3 - \mu - z_r^{-1} - z_{r-1}^{-1} - b(\tilde{T}(r))^{-1} = 0.$$

Since $b(\tilde{T}(r)) < 0$, Equation (30) shows that $z_r < (\sqrt{5}-1)/2$. By expressing $a_{\tilde{v}}(\tilde{T}(r))$ only in terms of z_r and μ, we discover that z_r is the only root of

$$g_\mu(x) = (4 - 5\mu + \mu^2)x^2 - (1 + 3\mu - \mu^2)x^2 - (6 - 6\mu + \mu^2)x + 3 - \mu$$

belonging to the interval $(0, 1)$. In fact, the polynomial has a negative root, $g_\mu(0) > 0$ and $g_\mu(1) = -\mu(3-\mu) < 0$. We also deduce that the function $g_\mu(x)$ is positive for $x \in (0, z_r)$ and negative for $x \in (z_r, 1)$.
When $r \to \infty$, z_r tends to $z_\infty = (\sqrt{57}-3)/8$, which is the smallest positive root of $g_0(x)$. We observe that $z_r > z_\infty$ since the number

$$g_\mu(z_\infty) = \frac{\mu}{128}\left((45 - 7\sqrt{57})\mu + 27\sqrt{57} - 137\right)$$

is positive.
We now execute $\tilde{D}'$:=*Diagonalize*($\tilde{T}'(r), -\mu$). The proof will be over once we show that D' has at least two negative outputs. We already know that $z_i > 0$ for all $i \leqslant r+1$. Let $b(\tilde{T}'(r))$ and $c(\tilde{T}'(r))$ denote the outputs of D' in correspondence of the two vertices of degree 3 (see Fig. 13). We have

$$b(\tilde{T}'(r)) = b(\tilde{T}(r)) = 3 - \mu - 2z_{r+1}^{-1} < 0.$$

On the contrary,

$$c(\tilde{T}'(r)) = 3 - \mu - 2z_{r-1}^{-1} = 2z_r + \mu - 1$$

is positive, since $z_r > z_\infty > 0.568 > (1-\mu)/2$. The last step consists in showing that $a_{\tilde{v}}(\tilde{T}'(r)) = 2 - \mu - b(\tilde{T}'(r))^{-1} - c(\tilde{T}'(r))^{-1}$ is negative. After some calculations, it turns out that

$$a_{\tilde{v}}(\tilde{T}'(r)) = -\frac{\Upsilon_\mu(z_r)}{(2z_r + \mu - 1)(3 - \mu - z_r(4 - 5\mu + \mu^2))}$$

where the denominator is positive and

$$\Upsilon_\mu(x) = 2(2-\mu)(3-5\mu+\mu^2)x^2 - (20-34\mu+23\mu^2-8\mu^3+\mu^4)x+8-11\mu+6\mu^2-\mu^3.$$

For $0 < \mu < 0.18216$, $\Upsilon_\mu(x)$ is a facing up parabola with two positive roots. Furthermore, $\Upsilon_\mu(0) > 0$, $\Upsilon_\mu(1) < 0$, and

$$\Upsilon_\mu\left(\frac{\sqrt{5}-1}{2}\right) = \frac{1}{2}\cdot\Big(72-32\sqrt{5}-2(30\sqrt{5}-67)\mu-(37\sqrt{5}-77)\mu^2 \\ +2(5\sqrt{5}-8)\mu^3-(\sqrt{5}-1)\mu^4\Big) > 0$$

This implies that $\Upsilon_\mu(x)$ is always positive in the interval $(0, (\sqrt{5}-1)/2)$. In particular, it is positive when evaluated in z_r. □

The remaining two propositions compare the algebraic connectivity of H-shape trees with $4r+5$ vertices.

Proposition 5.9. For each $r \geqslant 1$, $\mu_2(H^2_{r+1,r+1,r+1,r}) > \mu_2(H^2_{r+2,r+1,r,r})$.

Proof. For $r \in \{2,3\}$ the statement comes from a direct computation. Let $r \geqslant 4$. We set $T(r) := H^2_{r+1,r,r+1,r+1}$ (this notation suggests that the chosen root is adjacent to H-rays of different length), $T'(r) := H^2_{r+1,r+1,r-1,r-2}$, and $\mu := \mu(T(r))$. The proof initially requires the execution of $D :=$*Diagonalize*$(T(r), -\mu)$. Since $T(4) \subseteq T(r)$, $\mu := \mu_2(T(r)) < \mu_2(T(4)) = 0.06162 < 0.07$. Since D produces just one negative output, $z_i > 0$ for $1 \leqslant i \leqslant r+1$, and the root value $a_{\tilde{v}}(T(r))$ is zero.
As a consequence of Lemma 5.2 the numbers

$$\hat{b} = 3-\mu-2z_{r+1}^{-1} \quad \text{and} \quad \hat{a} = 3-\mu-z_r^{-1}-z_{r+1}^{-1}$$

cannot be both zero. The number $\hat{a}$ would compute the root value $a_{\tilde{v}}(T(r))$ if it were zero $\hat{b}$, the first number computed by the algorithm in correspondence of the non-root of degree 3. In other words, we surely have

$$b = \hat{b} < 0 \quad \text{and} \quad a_{\tilde{v}}(T(r)) = \hat{a} - b^{-1} = 0.$$

Replacing $-z_r^{-1}$ with $z_{r+1}-2+\mu$ in the equation $b^{-1} = \hat{a}$, we arrive at $b = z_{r+1}(z_{r+1}^2 + z_{r+1}-1)^{-1}$. Knowing that b is negative, we discover that $0 < z_{r+1} < \hat{q} := (\sqrt{5}-1)/2$. Furthermore, by equating

$$3-\mu-\frac{2}{z_{r+1}} = \frac{z_{r+1}}{z_{r+1}^2+z_{r+1}-1},$$

it turns out that z_{r+1} is the unique root of the polynomial

$$h_\mu(x) = (3-\mu)x^3 - \mu x^2 - (5-\mu)x + 2$$

in the interval $(0, \hat{q})$; in fact, the Descartes' rule of signs says that $h_\mu(x)$ has two positive roots, and precisely one of them is larger than $\hat{q}$ since $h_\mu(0) = 2$ and $h_\mu(\hat{q}) = -(3-\sqrt{5})/2$.

We now execute D':=*Diagonalize*$(T'(r), -\mu)$. We already realized that $z_i > 0$ for $i \leqslant r+1$, whereas

$$z_{r+2} = 2 - \mu - z_{r+1}^{-1} < 0 \quad \iff z_{r+1} < (2-\mu)^{-1},$$

and the latter is precisely the case since

$$h_\mu\left(\frac{1}{2-\mu}\right) = 1 - \frac{9 - 9\mu + 2\mu^2}{(2-\mu)^3}$$

is negative for $\mu \in (0,1)$. The proof ends once we show that D' has at least a second negative output. Let us compute

$$b(T') = 3 - \mu - 2z_r^{-1} = 3 - \mu + 2(z_{r+1} - (2-\mu)) = 2z_{r+1} - (1-\mu).$$

This number is negative, since

$$h_\mu\left(\frac{1-\mu}{2}\right) = -\frac{1 - 12\mu - 12\mu^2 + 8\mu^3 - \mu^4}{8}$$

is negative for $\mu < 0.07$, implying that $z_{r+1} < (1-\mu)/2$. □

The H-shape trees involved in Propositions 5.6 and 5.9 are obtained one from another through a graph perturbation called *shifting* in [8], yet the sufficient conditions on the Fiedler vector considered in [8, Lemma 7] guaranteeing the inequality in the two statements does not hold.

Proposition 5.10. For each $r \geqslant 1$, $\mu_2(H^2_{r+1,r+1,r+1,r}) > \mu_2(H^3_{r+1,r+1,r,r})$.

Proof. For $r \in \{2,3\}$ the statement comes from direct computations. Let now $r \geqslant 4$, $\mu := \mu_2(H^2_{r+1,r+1,r+1,r})$ and $T''(r) = H^3_{r+1,r+1,r,r}$ (see the H-shape tree on the right in Fig. 13). In order to execute the algorithm D'' :=*Diagonalize*$(T''(r), -\mu)$, we acquire several data from the proof of Proposition 5.9. We know that $z_i > 0$ for all $i \leqslant r+1$, $3 - \mu - 2z_r^{-1} < 0$ and $3 - \mu - 2z_{r+1}^{-1} < 0$. Since the latter two numbers are the output values processed by D'' for $b(T''(r))$ and $c(T''(r))$ (see Fig. 13), the algorithm D'' has (at least) two negative outputs, proving the statement. □

Acknowledgements

The authors express deep gratitude and appreciation to the anonymous referee for his/her careful reading and constructive comments. His/her suggestions helped us to better organize the material.

References

[1] S. Akbari, F. Belardo, F. Heydari, M. Maghasedi, and M. Souri, *On the largest eigenvalue of signed unicyclic graphs*, Linear Algebra Appl. **581** (2019), 145–162.

[2] S. Akbari, S. Dalvandi, F. Heydari, and M. Maghasedi, *Signed complete graphs with maximum index*, Discuss. Math. Graph Theory **40**, no. 2, 393–403.

[3] F. Belardo, M. Brunetti, and A. Ciampella, *Signed bicyclic graphs minimizing the least laplacian eigenvalue*, Linear Algebra Appl. **557** (2018), 201–233.

[4] ______, *Unbalanced unicyclic and bicyclic graphs with extremal spectral radius*, Czechoslovak Math. J. **71** (2021), no. 2, 417–433.

[5] F. Belardo, M. Brunetti, V. Trevisan, and J.-F. Wang, *On Quipus whose signless Laplacian index does not exceed* 4.5, (submitted).

[6] F. Belardo, E.M. Li Marzi, and S.K. Simić, *Combinatorial approach for computing the characteristic polynomial of a matrix*, Linear Algebra Appl. **433** (2010), no. 8-10, 1513–1523.

[7] F. Belardo and Y. Zhou, *Signed graphs with extremal least laplacian eigenvalue*, Linear Algebra Appl. **497** (2016), 167–180.

[8] T. Bıyıkoğlu and J. Leydold, *Graphs of given order and size and minimum algebraic connectivity*, Linear algebra Appl. **436** (2012), no. 7, 2067–2077.

[9] M. Brunetti and Z. Stanić, *Ordering signed graphs with large index*, (submitted).

[10] ______, *Unbalanced signed graphs with extremal spectral radius or index*, (submitted).

[11] D. Cvetković, P. Rowlinson, and S.K. Simić, *Signless Laplacians of finite graphs*, Linear Algebra Appl. **423** (2007), no. 1, 155–171.

[12] D.M. Cvetković, M. Doob, and H. Sachs, *Spectra of Graphs – Theory and Application*, 3rd edition, Johann Ambrosius Barth Verlag, Heidelberg-Leipzig, 1995.

[13] E. Ghorbani and A. Majidi, *Signed graphs with maximal index*, Discrete Math. **344** (2021), no. 8, 112463.

[14] C. He, Y. Li, H. Shan, and W. Wang, *On the index of unbalanced signed bicyclic graphs*, Comput. Appl. Math. **40** (2021), no. 4, 1–14.

[15] D.P. Jacobs and V. Trevisan, *Locating the eigenvalues of trees*, Linear Algebra Appl. **434** (2011), no. 1, 81–88.

[16] C.R. Johnson and B.D. Sutton, *Hermitian matrices, eigenvalue multiplicities, and eigenvector components*, SIAM J. Matrix Anal. Appl. **26** (2004), no. 2, 390–399.

[17] T. Koledin and Z. Stanić, *Connected signed graphs of fixed order, size, and number of negative edges with maximal index*, Linear Multilinear Algebra **65** (2017), no. 11, 2187–2198.

[18] K.L. Patra and A.K. Lal, *The effect on the algebraic connectivity of a tree by grafting or collapsing of edges*, Linear Algebra Appl. **428** (2008), no. 4, 855–864.

[19] M. Souri, F. Heydari, and M. Maghasedi, *Maximizing the largest eigenvalues of signed unicyclic graphs*, Discrete Math. Algorithms Appl. **12** (2020), no. 2, ID: 2050016.

[20] Z. Stanić, *Integral regular net-balanced signed graphs with vertex degree at most four*, Ars Math. Contemp. **17** (2019), no. 1, 103–114.

[21] T. Zaslavsky, *Signed graphs*, Discrete Appl. Math. **4** (1982), no. 1, 47–74.

Appendix: Indices of small graphs in $\mathfrak{B}_n^*$

Table 1. **Indices of graphs of type (2) up to 10 vertices.**

n	5	6	7	8	9	10
Γ	$\Phi_{0,5}$	$\Phi_{1,2}$	$\Phi_{1,3}$	$\Phi_{1,4}$	$\Phi_{1,5}$	$\widetilde{\Phi}_{2,2}$
λ_1	$\frac{\sqrt{17}-1}{2}$	1.67828	1.69353	1.76893	1.79129	1.81784

Table 2. **Indices of some 'small' graphs considered along the paper**

Graph	λ_1	Graph	λ_1	Graph	λ_1	Graph	λ_1
$n=5$		$n=7$		$n=8$		$n=8$ (continuation)	
$\Phi_{0,1}$	1.56155	$\Phi_{1,3}$	1.69353	$\Phi_{1,3}$	1.76893	Θ_{11}	1.97446
$\Delta_{1,0}$	1.74912	Γ_1	1.90321	Γ_2	1.96607	Θ_{15}	1.97121
		Γ_5	1.94242	Γ_3	1.97722	Θ_{16}	1.97597
		Γ_{10}	1.95546	Γ_4	1.98010	Θ_{17}	1.97722
$n=6$		Γ_{13}	1.96202	Γ_6	1.97280	Θ_{26}	1.96255
$\Phi_{1,2}$	1.67828	Θ_2	1.87939	Γ_7	1.97926	Θ_{27}	1.97086
Γ_9	1.90321	Θ_6	1.90211	Γ_8	1.98166	Θ_{28}	1.97280
$\Lambda^1_{0,0;0}$	1.81361	Θ_{12}	1.92103	Γ_{11}	1.98227	Θ_{29}	1.98011
$\Gamma^2_{0,0,0,0}$	$\sqrt{3}$	Θ_{13}	1.93230	Γ_{12}	1.98407	Θ_{30}	1.98237
Θ_5	$\sqrt{3}$	Θ_{14}	1.93543	Γ_{14}	1.98595	Θ_{31}	1.95197
Θ_{18}	1.84943	Θ_{20}	1.87939	Γ_{15}	1.98708	Θ_{32}	1.97825
Θ_{19}	1.87112	Θ_{21}	1.92022	Γ_{16}	1.98552	Θ_{33}	1.98095
Θ_{34}	1.89420	Θ_{22}	1.93543	$\Lambda^1_{1,1;0}$	1.89761	Θ_{38}	1.97908
$\Delta_{1,1}$	1.79129	Θ_{23}	1.94011	Θ_1	1.95630	Θ_{39}	1.98460
$\Delta_{2,0}$	1.85133	Θ_{24}	1.94551	Θ_3	1.93894		
$\Delta'_{1,1}$	1.90321	Θ_{25}	1.94781	Θ_4	1.95069		
$\Delta'_{2,0}$	1.86620	Θ_{35}	1.94341	Θ_7	1.95630		
		Θ_{36}	1.95423	Θ_8	1.96962		
		Θ_{37}	1.95546	Θ_9	1.96884		
				Θ_{10}	1.97230		